Speciation and Mechanistic Studies of Chiral Copper(I) Schiff Base Precursors Mediating Asymmetric Carbenoid Insertion Reactions of Diazoacetates into the Si−H Bond of Silanes

Les A. Dakin,[†] Patricia C. Ong,[†] James S. Panek,*[,†] Richard J. Staples,[‡] and Pericles Stavropoulos*[,†]

Department of Chemistry, Boston University, Boston, Massachusetts 02215, and Department of Chemistry and Chemical Biology, Harvard University, Cambridge, Massachusetts 02138

Received May 3, 2000

$[Cu(CH_3CN)_4](PF_6)$ and the chiral C_2-symmetric diimine ligand (1*R*,2*R*)-bis((2,6-dichlorobenzylidene)diamino)cyclohexane (*R*,*R*-**1**) (1.2 equiv) mediate asymmetric carbenoid insertion of aryl diazoesters into the Si−H bond of silanes in good to high yields and levels of enantiocontrol. Dichloromethane solutions of $[Cu(CH_3CN)_4](PF_6)$/*R*,*R*-**1** afford yellow crystals of $[Cu^I(R,R\text{-}\mathbf{1})(CH_3CN)\cdot Cu^I(R,R\text{-}\mathbf{1})(CH_3CN)_2\cdot Cu^I_2(R,R\text{-}\mathbf{1})_3](PF_6)_4\cdot 2CH_2Cl_2\cdot 3Et_2O$, which feature three distinct copper complexes in the crystal lattice. ^{1}H NMR and electrospray ionization MS (ESI-MS) studies establish that only $[Cu^I(R,R\text{-}\mathbf{1})(CH_3CN)]^+$ is present in solution in high yields. Upon addition of stoichiometric $PhC(N_2)CO_2Me$, cations $[Cu^I(R,R\text{-}\mathbf{1})(C(CO_2Me)Ph)]^+$ and $[Cu^I(R,R\text{-}\mathbf{1})(C(CO_2Me)Ph)(CH_3CN)]^+$ are detected by ESI-MS, consistent with the presence of a copper−carbenoid moiety. The catalytically active precursor is most likely a mononuclear unit of the type $[Cu^I(R,R\text{-}\mathbf{1})(CH_3CN)_n]^+$, as suggested by the linearity of plots relating the enantiomeric excess (ee) of product to that of the ligand (Kagan's analysis). Hammett plots correlate enhanced catalytic reactivities with stabilization of a sizable positive charge on the carbenoid carbon and a smaller positive charge on the silicon atom, but the corresponding enantioselectivities are insensitive to these electronic properties. The kinetic isotope effect for carbenoid insertion into $PhMe_2Si-H(D)$ varies from 2.12 (−40 °C) to 1.08 (25 °C), in agreement with other small KIE values observed for processes in which Si−H activation is involved in the turnover-limiting step. A linear Eyring plot of ln(*k*(major enantiomer)/*k*(minor enantiomer)) over a range of 80 K supports the notion of a single step controlling the levels of enantioselection. No H/D scrambling is observed in competitive carbenoid insertions into $PhMe_2Si\text{-}D/Ph_2MeSi\text{-}H$, indicating that the insertion reaction takes place in a concerted fashion. These results are discussed in light of an early transition state, characterized by hydrogen-first penetration of the Si−H bond into the copper−carbenoid cavity, which is assumed to impart high levels of enantioselectivity due to intrinsic preorganization under the influence of the specific ligand and aryl diazoesters employed.

Introduction

The selective activation of unfunctionalized C−H[1] and Si−H[2] bonds is a transformation of great synthetic potential and utility. Of particular interest are methodologies[3] that involve insertion of a metal-activated electrophilic moiety into a C−H or Si−H bond under high levels of regio-, diastereo-, or enantiocontrol. Electrophilic metal−carbene species,[4] generated in situ via decomposition of α-diazocarbonyl compounds,[5] have been known to mediate both intra- and intermolecular[6] carbenoid C−H and Si−H insertion reactions, as well as ylide type "insertions" into N−H, O−H, and S−H bonds[7] (eq 1).

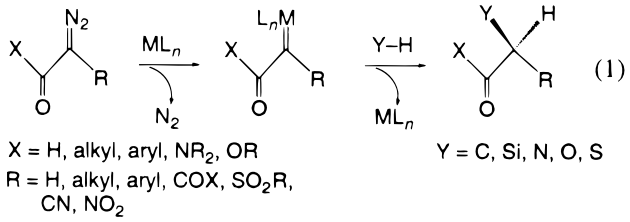

(1)

The most prominent metal-centered reagents in this context are dirhodium(II) carboxylate and carboxami-

[†] Boston University.
[‡] Harvard University.

(1) (a) Arndtsen, B. A.; Bergman, R. G.; Mobley, T. A.; Peterson, T. H. *Acc. Chem. Res.* **1995**, *28*, 154−162. (b) Olah, G. A.; Prakash, G. K. S. In *The Chemistry of Alkanes and Cycloalkanes*; Patai, S., Rappoport, Z., Eds.; John Wiley & Sons: New York, 1992; pp 609−652. (c) Shilov, A. E.; Shul'pin, G. *Chem. Rev.* **1997**, *97*, 2879−2932.

(2) (a) Ojima, I.; Li, Z.; Zhu, J. In *The Chemistry of Organic Silicon Compounds*; Rappoport, Z., Apeloig, Y., Eds.; John Wiley & Sons: New York, 1998; Vol. 2, Part 2, pp 1687−1792. (b) Tilley, T. D. In *The Silicon-Heteroatom Bond*; Patai, S., Rappoport, Z., Eds.; John Wiley & Sons: New York, 1991; pp 245−364. (c) Corey, J. Y.; Braddock-Wilking, J. *Chem. Rev.* **1999**, *99*, 175−292.

(3) Doyle, M. P.; McKervey, M. A.; Ye, T. *Modern Catalytic Methods for Organic Synthesis with Diazo Compounds*; Wiley-Interscience: New York, 1998.

(4) (a) Doyle, M. P.; Forbes, D. C. *Chem. Rev.* **1998**, *98*, 911−935. (b) Doyle, M. P. *Chem. Rev.* **1986**, *86*, 919−939. (c) Padwa, A.; Austin, D. J. *Angew. Chem., Int. Ed. Engl.* **1994**, *33*, 1797−1815.

10.1021/om0003786 CCC: $19.00
Publication on Web 06/29/2000

date species, chiral versions of which have been shown[4] to induce remarkable levels of enantioselection in C−H and Si−H insertion reactions. Intermolecular insertion into C−H bonds[8] has proven to be particularly challenging, as evidenced by the only recently disclosed examples of highly selective, Rh(II)-catalyzed, asymmetric carbenoid insertion into the C−H bonds of cycloalkanes[9] (eq 2) or the α-C−H bonds of tetrahydrofuran and cyclic amines.[10]

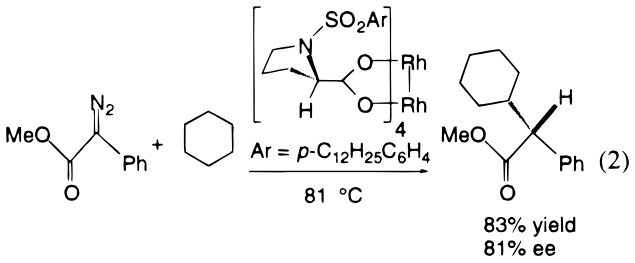

(2)

In contrast, asymmetric intramolecular carbenoid C−H insertion reactions have been widely demonstrated,[11] especially in synthetic methodology that requires formation of five-member heteroatom-containing rings[12] (eq 3).

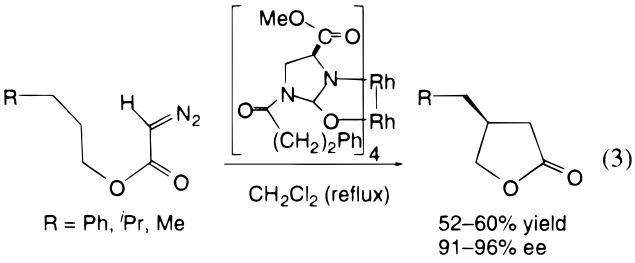

(3)

The more reactive Si−H bonds can readily undergo asymmetric intermolecular insertion reactions catalyzed by chiral Rh(II) carbenoid species,[7a,13] generated via decomposition of phenyl or vinyl diazoacetates (eq 4).

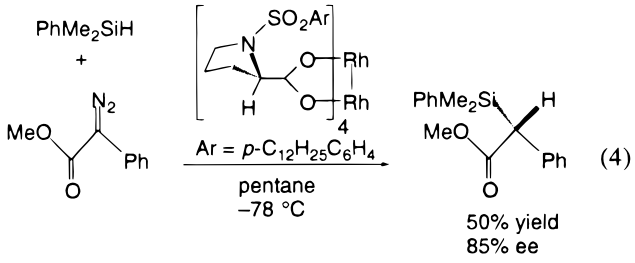

(4)

Currently emerging as more economical alternatives to rhodium-based reagents are chiral C_2-symmetric copper(I) diimine compounds, whose utility in mediating carbenoid (Cu=CRR′) or nitrenoid (Cu=NR) addition to unsaturated substrates has been amply demonstrated by Jacobsen's group in enantioselective cyclopropanation[14] (eq 5) and aziridination[14,15] (eq 6) reactions,

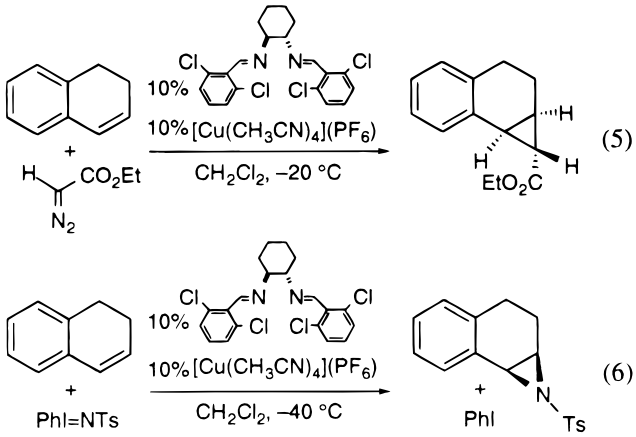

(5) (6)

respectively. Another major class of widely applicable C_2-symmetric chiral reagents constitutes the bis(oxazolinyl) (box) and bis(oxazolinyl)pyridyl (pybox) Cu(I) and Cu(II) systems, which have been developed by Masamune,[16] Evans,[17] and Pfaltz[18] to catalyze, inter alia, enantioselective cyclopropanation, Diels−Alder, and aldol reactions. These copper reagents have a close

(5) (a) Ye, T.; McKervey, M. A. *Chem. Rev.* **1994**, *94*, 1091−1160. (b) Brunner, H. *Angew. Chem., Int. Ed. Engl.* **1992**, *31*, 1183−1185.
(6) Davies, H. M. L. *Aldrichim. Acta* **1997**, *30*, 107−114.
(7) (a) Bulugahapitiya, P.; Landais, Y.; Parra-Rapado, L.; Planchenault, D.; Weber, V. *J. Org. Chem.* **1997**, *62*, 1630−1641, and references therein. (b) Simal, F.; Demonceau, A.; Noels, A. F. *Tetrahedron Lett.* **1999**, *40*, 63−66.
(8) (a) Adams, J.; Poupart, M.-A.; Greainer, L.; Schaller, C.; Quimet, N.; Frenette, R. *Tetrahedron Lett.* **1989**, *30*, 1749−1752. (b) Demonceau, A.; Noels, A. F.; Hubert, A. J.; Teyssie, P. *J. Mol. Catal.* **1988**, *49*, L13-L17. (c) Callott, H. J.; Metz, F. *Nouv. J. Chim.* **1985**, *9*, 167−171. (d) Demonceau, A.; Noels, A. F.; Hubert, A. J.; Teyssie, P. *Bull. Soc. Chim. Belg.* **1984**, *93*, 945−948. (e) Callott, H. J.; Metz, F. *Tetrahedron Lett.* **1982**, *23*, 4321−4324. (f) Demonceau, A.; Noels, A. F.; Hubert, A. J.; Teyssie, P. *J. Chem. Soc., Chem. Commun.* **1981**, 688−689. (g) Scott, L. T.; DeCicco, G. J. *J. Am. Chem. Soc.* **1974**, *96*, 322−323. (h) Ambramovitch, R. A.; Roy, J. *J. Chem. Soc., Chem. Commun.* **1965**, 542−543.
(9) (a) Davies, H. M. L.; Hansen, T. *J. Am. Chem. Soc.* **1997**, *119*, 9075−9076. (b) Davies, H. M. L.; Hodges, L. M.; Matasi, J. J.; Hansen, T.; Stafford, D. G. *Tetrahedron Lett.* **1998**, *39*, 4417−4420.
(10) Davies, H. M. L.; Hansen, T.; Hopper, D. W.; Panaro, S. A. *J. Am. Chem. Soc.* **1999**, *121*, 6509−6510.
(11) Doyle, M. P. In *Comprehensive Organometallic Chemistry II*; Hegedus, L. S., Ed.; Pergamon Press: New York, 1995; Vol. 12, Chapters 5.1 and 5.2.
(12) (a) Doyle, M. P.; Kalinin, A. V.; Ene, D. G. *J. Am. Chem. Soc.* **1996**, *118*, 8837−8846. (b) Bode, J. W.; Doyle, M. P.; Protopopova, M. N.; Zhou, Q.-L. *J. Org. Chem.* **1996**, *61*, 9146−9155. (c) Doyle, M. P.; Dyatkin, A. B.; Roos, G. H. P.; Cañas, F.; Pierson, D. A.; van Basten, A.; Müller, P.; Polleux, P. *J. Am. Chem. Soc.* **1994**, *116*, 4507−4508. (d) Doyle, M. P.; Westrum, L. J.; Wolthuis, W. N. E.; See, M. M.; Boone, W. P.; Bagheri, V.; Pearson, M. M. *J. Am. Chem. Soc.* **1993**, *115*, 958−964. (e) Taber, D. F.; You, K. K.; Rheingold, A. L. *J. Am. Chem. Soc.* **1996**, *118*, 547−556. (f) Taber, D. F.; Song, Y. *J. Org. Chem.* **1996**, *61*, 6706−6712. (g) Wang, P.; Adams, J. *J. Am. Chem. Soc.* **1994**, *116*, 3296−3305.
(13) (a) Davies, H. M. L.; Hansen, T.; Rutberg, J.; Bruzinski, P. R. *Tetrahedron Lett.* **1997**, *38*, 1741−1744. (b) Buck, R. T.; Doyle, M. P.; Drysdale, M. J.; Ferris, L.; Forbes, D. C.; Haigh, D.; Moody, C. J.; Pearson, N. D.; Zhou Q.-L. *Tetrahedron Lett.* **1996**, *37*, 7631−7634. (c) Landais, Y.; Parra-Rapado, L.; Planchenault, D.; Weber, V. *Tetrahedron Lett.* **1997**, *38*, 229−232. (d) Landais, Y.; Planchenault, D. *Tetrahedron Lett.* **1994**, *35*, 4565−4568.
(14) Li, Z.; Quan, R. W.; Jacobsen, E. N. *J. Am. Chem. Soc.* **1995**, *117*, 5889−5890.
(15) Li, Z.; Conser, K. R.; Jacobsen, E. N. *J. Am. Chem. Soc.* **1993**, *115*, 5326−5327.
(16) (a) Lowenthal, R. E.; Abiko, A.; Masamune, S. *Tetrahedron Lett.* **1990**, *31*, 6005−6008. (b) Lowenthal, R. E.; Masamune, S. *Tetrahedron Lett.* **1991**, *32*, 7373−7376.
(17) (a) Evans, D. A.; Woerpel, K. A.; Hinman, M. M.; Faul, M. M. *J. Am. Chem. Soc.* **1991**, *113*, 726−728. (b) Evans, D. A.; Miller, S. J.; Lectka, T. *J. Am. Chem. Soc.* **1993**, *115*, 6460−6461. (c) Evans, D. A.; Faul, M. M.; Bilodeau, M. T. *J. Am. Chem. Soc.* **1994**, *116*, 2742−2753. (d) Evans, D. A.; Kozlowski, M. C.; Burgey, C. S.; MacMillan, D. W. C. *J. Am. Chem. Soc.* **1997**, *119*, 7893−7894. (e) Evans, D. A.; Johnson, J. S. *J. Am. Chem. Soc.* **1998**, *120*, 4895−4896. (f) Evans, D. A.; Burgey, C. S.; Paras, N. A.; Vojkovsky, T.; Tregay, S. W. *J. Am. Chem. Soc.* **1998**, *120*, 5824−5825.
(18) (a) Müller, D.; Umbricht, G.; Weber, B.; Pfaltz, A. *Helv. Chim. Acta* **1991**, *74*, 232−240. (b) Pfaltz, A. *Adv. Catal. Proc.* **1995**, *1*, 61−94.

precedent in Pfaltz's chiral Cu(II)−semicorrin systems.[19] Notable is also the class of Cu(I) reagents with C_2-symmetric bisazaferrocene ligands introduced by Fu.[20]

The presumed generation of a distinct copper carbene or copper nitrene intermediate, situated preferentially at a mononuclear copper site, has provided a unifying mechanistic hypothesis[14] to account for comparable levels of stereocontrol between cyclopropanation and aziridination reactions, catalyzed by any given member of the chiral copper diimine class of compounds. Assuming that incipient formation of a copper carbene intermediate is also responsible for insertion reactions, as generally accepted[12d] for similar dirhodium(II)-based carbenoid insertions into C−H and Si−H bonds, a mechanistic scenario of wide applicability is then emerging that can be conveniently tested on the same class of chiral C_2-symmetric copper diimine compounds.

A preliminary report[21] from our laboratories in collaboration with Jacobsen's group demonstrated that these copper catalysts can induce good to high yields of enantioselection in carbenoid Si−H insertion reactions, albeit restricted to the aryldiazoacetate class of α-diazocarbonyl precursors (eq 7). In the present article, we

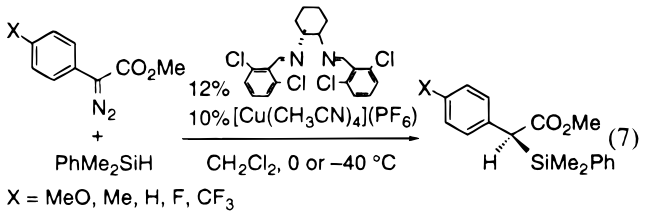

examine in detail structural and mechanistic aspects of the copper-mediated Si−H insertion reaction to reveal unanticipated level of complexity in the speciation of the chiral copper diimine species in solution. Despite this complexity, several mechanistic indicators are consistent with the notion that a mononuclear site is responsible for the generation of a metal carbenoid precursor which performs genuine insertion into the Si−H bond of aryl and alkyl silanes, most likely featuring an early transition state that retains elements of hydride transfer character.

Experimental Section

General Considerations. Unless otherwise stated, all operations involving synthesis and characterization of copper reagents were performed under a pure dinitrogen or argon atmosphere, using Schlenk techniques on an inert gas/vacuum manifold or in a drybox (O_2, H_2O < 2 ppm). Hexane, petroleum ether, and toluene were distilled over Na; THF and diethyl ether, over Na/Ph_2CO. Acetonitrile and methylene chloride were distilled over CaH_2. Ethanol and methanol were distilled over the corresponding magnesium alkoxide, and acetone was distilled over drierite. Deuterated solvents for NMR experiments were purchased from Cambridge Isotope Laboratory. All solvents, with the exception of methanol and water, were degassed by three freeze−pump−thaw cycles. Methanol and water were degassed by bubbling nitrogen or argon for 0.5 h. Starting materials were purchased from Aldrich and are of the highest available purities. $[Cu(CH_3CN)_4](PF_6)$ was freshly prepared prior to use from Cu_2O and HPF_6 according to a procedure by Kubas.[22] Analytical thin-layer chromatography was performed on Whatman Reagent 0.25 mm silica gel 60-A plates. Flash chromatography was performed on E. Merck silica gel 230−400 mesh. Enantiomeric excess (ee) values were determined by chiral HPLC (Chiralcel OD) with hexanes/isopropyl alcohol (98:2) as the mobile phase with a flow rate of 1 mL/min at 254 nm.

$[Cu^I(R,R\text{-}1)(CH_3CN)\cdot Cu^I(R,R\text{-}1)(CH_3CN)_2\cdot Cu^I_2(R,R\text{-}1)_3](PF_6)_4\cdot 2CH_2Cl_2\cdot 3Et_2O$ (2). $[Cu(CH_3CN)_4](PF_6)$ (200 mg, 0.54 mmol) and *R,R*-**1**[23] (274 mg, 0.64 mmol) were dissolved in CH_2Cl_2 (30.0 mL) and stirred for 10 min. The yellow solution was filtered, and the filtrare was reduced under vacuum to 5 mL. Diffusion of diethyl ether into this solution at −10 °C provides initially a small amount (10 mg, 4.5%) of colorless crystals of $[Cu(CH_3CN)_4](PF_6)\cdot CH_3CN$, which were filtered off. Diffusion of excess diethyl ether into the filtrate affords yellow crystals of **2** (370 mg, 78.5%). ^1H NMR (CD_2Cl_2): δ 8.473 (s, 2H, *H*C=N), 7.412 (q, 6H, Ph), 3.540 (dd, 2H, N−C*H* (cy), 2.437 (d, 2H, cy), 2.044 (d, 2H, cy), 1.938 (s, 3H, CH_3CN), 1.608 (m, 2H, cy), 1.466 (m, 2H, cy). Anal. Calcd for $C_{120}H_{133}N_{13}Cl_{24}Cu_4F_{24}O_3P_4$: C, 41.29; H, 3.84; N, 5.22; Cl, 24.38; F, 13.06; P, 3.55. Found: C, 41.82; H, 3.79; N, 5.18; Cl, 24.89; F, 13.33; P, 3.43.

Representative Procedure for Asymmetric Carbenoid Insertion into the Si−H Bond. (2*S*)-Methyl (1-phenyl-2-dimethylphenylsilyl)propanoate (3). To a round-bottom

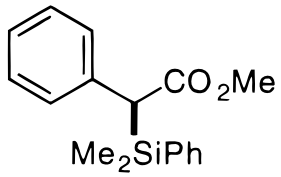

flask charged with a stir bar is added $[Cu(CH_3CN)_4](PF_6)$ (53 mg, 0.142 mmol) and the dichlorodiimine ligand *R,R*-**1** (73 mg, 0.170 mmol). The mixture was dissolved in dry CH_2Cl_2 (4.5 mL), and the resulting homogeneous yellow solution was allowed to react at room temperature for 30 min. To this solution was added via syringe phenyldimethylsilane (388 mg, 2.85 mmol). The resulting solution was allowed to stir for 10 min at room temperature before being cooled to −40 °C. To the cooled reaction mixture was added dropwise a solution of $PhC(N_2)CO_2Me$ (251 mg, 1.42 mmol) in CH_2Cl_2 (1.4 mL). The resulting mixture was allowed to stir at −40 °C for 48−72 h before being diluted with 10% ethyl acetate/hexanes and flushed through a thin pad of SiO_2. The resulting solution was then concentrated under vacuum to yield crude insertion product (**3**). The crude product was purified by SiO_2 chromatography using 2.5% ethyl acetate/hexanes as eluant, yielding **3** as a colorless oil (347 mg, 1.22 mmol, 86% yield). HPLC: t_R minor 4.33 min, t_R major 10.14 min. ^1H NMR (400 MHz, $CDCl_3$): δ 7.42−7.25 (m, 9H, Ar−*H*), 7.18 (m, 1H, Ar−*H*), 3.64 (s, 1H, C*H*), 3.58 (s, 3H, CO_2CH_3), 0.380 (s, 3H, Si−CH_3), 0.360 (S, 3H, Si−CH_3). ^{13}C NMR (67.5 MHz, $CDCl_3$): δ 173.05, 133.94, 133.89, 129.56, 128.28, 127.98, 127.62, 127.56, 125.61, 51.23, 45.95, −4.18, −4.60. IR (neat): ν_{max} 3528, 3026, 2952, 1955, 1600 cm^{-1}. CIMS (NH_3 gas): 284.1, 207.1, 135.1, 118.0, 89.0. CIHRMS: calcd for $[C_{17}H_{20}O_2Si + H]^+$ 284.1232, found 284.1298. $[\alpha]^{23}_D = -19.09°$ (c = 1.21, $CHCl_3$).

Analytical data for all other products of carbenoid insertion into Si−H bonds discussed in the text have been deposited as Supporting Information.

General Procedure for the Generation of Hammett Plots. (a) Para-Substituted Phenyl Diazoesters. The

(19) (a) Fritschi, H.; Leutenegger, U.; Pfaltz, A. *Angew. Chem., Int. Ed. Engl.* **1986**, *25*, 1005−1006. (b) Fritschi, H.; Leutenegger, U.; Siegmann, K.; Pfaltz, A.; Keller, W.; Kratky, C. *Helv. Chim. Acta* **1988**, *71*, 1541−1552. (c) Fritschi, H.; Leutenegger, U.; Pfaltz, A. *Helv. Chim. Acta* **1988**, *71*, 1553−1565. (d) Leutenegger, U.; Umbricht, G.; Fahrni, C.; von Matt, P.; Pfaltz, A. *Tetrahedron* **1992**, *48*, 2143-2156.

(20) Lo, M. M.-C.; Fu, G. C. *J. Am. Chem. Soc.* **1998**, *120*, 10270−10271.

(21) Dakin, L. A.; Schaus, S. E.; Jacobsen, E. N.; Panek, J. S. *Tetrahedron Lett.* **1998**, *39*, 8947−8950.

(22) Kubas, G. J. *Inorg. Synth.* **1979**, *19*, 90−92.

following is a typical procedure for determining the relative reactivity of *p*-X-PhC(N_2)CO_2Me (X = MeO, Me, F, CF_3) versus PhC(N_2)CO_2Me in carbenoid insertion reactions into the Si−H bond of $PhMe_2Si$−H. To a round-bottom flask charged with a stir bar is added [Cu(CH_3CN)$_4$](PF_6) (18 mg, 0.049 mmol) and the dichlorodiimine ligand *R*,*R*-**1** (25 mg, 0.059 mmol). The mixture was dissolved in dry CH_2Cl_2 (4.5 mL), and the resulting homogeneous yellow solution was allowed to react at room temperature for 30 min. To this solution was added via syringe phenyldimethylsilane (67 mg, 0.495 mmol). The resulting solution was allowed to stir for 10 min at room temperature before being cooled to 0 °C. To the cooled reaction mixture was added dropwise a solution of *p*-MeO-PhC(N_2)CO_2-Me (100 mg, 0.495 mmol) and PhC(N_2)CO_2Me (87 mg, 0.495 mmol) in CH_2Cl_2 (1.4 mL). The reaction was allowed to run until completion (TLC) and was diluted with cold 10% ethyl acetate/hexanes. This crude reaction mixture was subjected to a short silica gel plug to remove the copper reagent and was concentrated under vacuum. The ratio of the products (*p*-MeO/H) was determined through analysis of the crude reaction mixture using ^{1}H NMR spectroscopy.

(b) Para-Substituted Aryl Silanes. The following is a typical procedure for determining the relative reactivity of *p*-X-$PhMe_2SiH$ (X = MeO, Me, F, CF_3) versus $PhMe_2SiH$ in carbenoid insertion reactions of PhC(N_2)CO_2Me into the Si−H bond of the aryl silanes. To a round-bottom flask charged with a stir bar is added [Cu(CH_3CN)$_4$](PF_6) (28 mg, 0.074 mmol) and the dichlorodiimine ligand *R*,*R*-**1** (38 mg, 0.089 mmol). The mixture was dissolved in dry CH_2Cl_2 (4.5 mL), and the resulting homogeneous yellow solution was allowed to react at room temperature for 30 min. To this solution was added via syringe a mixture of *p*-MeO-$PhMe_2SiH$ (123 mg, 0.744 mmol) and $PhMe_2SiH$ (101 mg, 0.744 mmol). The resulting solution was allowed to stir for 10 min at room temperature before being cooled to 0 °C. To the cooled reaction mixture was added dropwise a solution of PhC(N_2)CO_2Me (131 mg, 0.744 mmol) in CH_2Cl_2 (1.4 mL). The reaction was allowed to run until completion (TLC) and was diluted with cold 10% ethyl acetate/hexanes. This crude reaction mixture was subjected to a short silica gel plug to remove the copper reagent and was concentrated under vacuum. The ratio of the products (*p*-MeO/H) was determined through analysis of the crude reaction mixture using ^{1}H NMR spectroscopy.

General Procedure for the Determinaton of the Kinetic Isotope Effect. Kinetic isotope effects (KIEs) were determined by dissolving equimolar amounts of H-$SiMe_2$Ph (283 mg, 2.08 mmol) and D-$SiMe_2$Ph (284 mg, 2.08 mmol) along with the copper complex [Cu(CH_3CN)$_4$](PF_6) (52 mg, 0.140 mmol) and the chiral diimine ligand *R*,*R*-**1** (72 mg, 0.168 mmol) in CH_2Cl_2 (4.5 mL) upon stirring. The reaction was then brought to the desired temperature using a cryogenic cooling bath, and PhC(N_2)CO_2Me (245 mg, 1.4 mmol) was introduced dropwise via syringe in CH_2Cl_2 (1.4 mL). The reaction was allowed to run until consumption of the phenyl diazoester (monitored by TLC) and was diluted with cold 10% ethyl acetate/hexanes. This crude reaction mixture was subjected to a short silica gel plug to remove the copper reagent and was concentrated under vacuum. The ratio of the products (H/D) was determined by ^{1}H NMR analysis of the crude reaction mixture with the assistance of authentic samples of the expected products.

X-ray Structure Determinations. Crystallographic data were determined for [Cu^I(CH_3CN)$_4$](PF_6)·CH_3CN (Supporting Information), [Cu^I(*R*,*R*-**1**)(CH_3CN)·Cu^I(*R*,*R*-**1**)(CH_3CN)$_2$·Cu^I_2(*R*,*R*-**1**)$_3$](PF_6)$_4$·2CH_2Cl_2·3Et_2O (**2**) (Table 1), and [Cu^I_2(*R*,*R*-**1**)$_3$](PF_6)$_2$·$PhSCO_2Et$·0.75CH_2Cl_2·0.5CH_3CN (Supporting Information). Single crystals were picked from the crystallization vessel (coated with Paratone-N oil if necessary due to air-sensitivity or desolvation), mounted on a glass fiber using grease, and transferred to a Siemens (Bruker) SMART CCD (charge coupled device) based diffractometer equipped with an LT-2 low-temperature apparatus operating at 213 K. Data were measured using omega scans of 0.3° per frame for 30 s, such that a hemisphere was collected. A total of 1271 frames were collected with a final resolution of 0.75 Å for [Cu^I(CH_3CN)$_4$](PF_6)·CH_3CN and [Cu^I_2(*R*,*R*-**1**)$_3$](PF_6)$_2$·$PhSCO_2Et$·0.75CH_2Cl_2·0.5CH_3CN, and 0.80 Å for **2**. The first 50 frames were recollected at the end of data collection to monitor for decay. Cell parameters were retrieved using SMART software[24] and refined using the SAINT software,[25] which corrects for *Lp* and decay. Absorption corrections were applied using SADABS[26] supplied by G. Sheldrick. The structures are solved by the direct method using the SHELXS-97[27] program and refined by least-squares methods on F^2, SHELXL-97,[28] incorporated in SHELXTL-PC V 5.10.[29]

Table 1. Crystallographic Data[a] for [Cu^I(*R*,*R*-1)(CH_3CN)·Cu^I(*R*,*R*-1)(CH_3CN)$_2$·Cu^I_2(*R*,*R*-1)$_3$](PF_6)$_4$·2CH_2Cl_2·3Et_2O (2)

formula	$C_{120}H_{133}Cl_{24}Cu_4F_{24}N_{13}O_3P_4$
fw	3490.24
cryst syst	orthorhombic
space group	*P*2(1)2(1)2(1)
Z	4
a, Å	18.0299(3)
b, Å	18.7372(5)
c, Å	44.781(1)
α, deg	90
β, deg	90
γ, deg	90
V, Å^3	15128.5(7)
T, K	213(2)
color	yellow
d_{calc}, g/cm^3	1.532
μ, mm^{-1}	1.102
GOF on F^2	1.031
R1[b] (wR2[c]), %	6.31 (7.90)

[a] Obtained with graphite-monochromated Mo Kα (*λ* = 0.71073 Å) radiation. [b] $R1 = \sum||F_o| - |F_c||/\sum|F_o|$. [c] $wR2 = \{\sum[w(F_o^2 - F_c^2)^2]/\sum[w(F_o^2)^2]\}^{1/2}$.

The structures were solved in the space groups specified in Table 1 and in the Supporting Information by analysis of systematic absences. All non-hydrogen atoms are refined anisotropically. Hydrogens were calculated by geometrical methods and refined as a riding model. The crystals used for the diffraction studies showed no decomposition during data collection. All drawings (Figures 1 and 2 and ORTEP diagrams in the Supporting Information) are done at 50% probability ellipsoids.

Other Physical Measurements. ^{1}H and ^{13}C NMR spectra were recorded on JEOL GSX-270 and Varian XL-400 NMR spectrometers. FT-IR spectra were obtained on a Perkin-Elmer 1800 spectrometer. UV−vis spectra were obtained on a Hewlett-Packard 8452A diode array spectrometer, equipped with an Oxford DN1704 cryostat and ITC4 temperature controller for low-temperature measurements. Electrospray ionization (ESI) mass spectra were recorded using a Platform II MS (Micromass Instruments, Danvers, MA). Samples were introduced from solutions specified in the text at a flow rate of 5 *μ*L/min from a syringe pump (Harvard Apparatus). The electrospray probe capillary was maintained at a potential of 3.0 kV, and

(23) Larrow, J. F.; Jacobsen, E. N.; Gao, Y.; Hong, Y.; Nie, X.; Zepp, C. M. *J. Org. Chem.* **1994**, *59*, 1939−1942.
(24) SMART V 5.050 (NT) *Software for the CCD Detector System*; Bruker Analytical X-ray Systems: Madison, WI, 1998.
(25) SAINT V 5.01 (NT) *Software for the CCD Detector System*; Bruker Analytical X-ray Systems: Madison, WI, 1998.
(26) SADABS *Program for Absorption Corrections Using Siemens CCD Based on the Method of Robert Blessing*: Blessing, R. H. *Acta Crystallogr.* **1995**, *A51*, 33−38.
(27) Sheldrick, G. M. *SHELXS-97 Program for the Solution of Crystal Structure*; University of Göttingen: Göttingen, Germany, 1997.
(28) Sheldrick, G. M. *SHELXL-97 Program for the Refinement of Crystal Structure*; University of Göttingen: Göttingen, Germany, 1997.
(29) *SHELXTL 5.10 (PC-Version) Program Library for Structure Solution and Molecular Graphics*; Bruker Analytical X-ray Systems: Madison, WI, 1998.

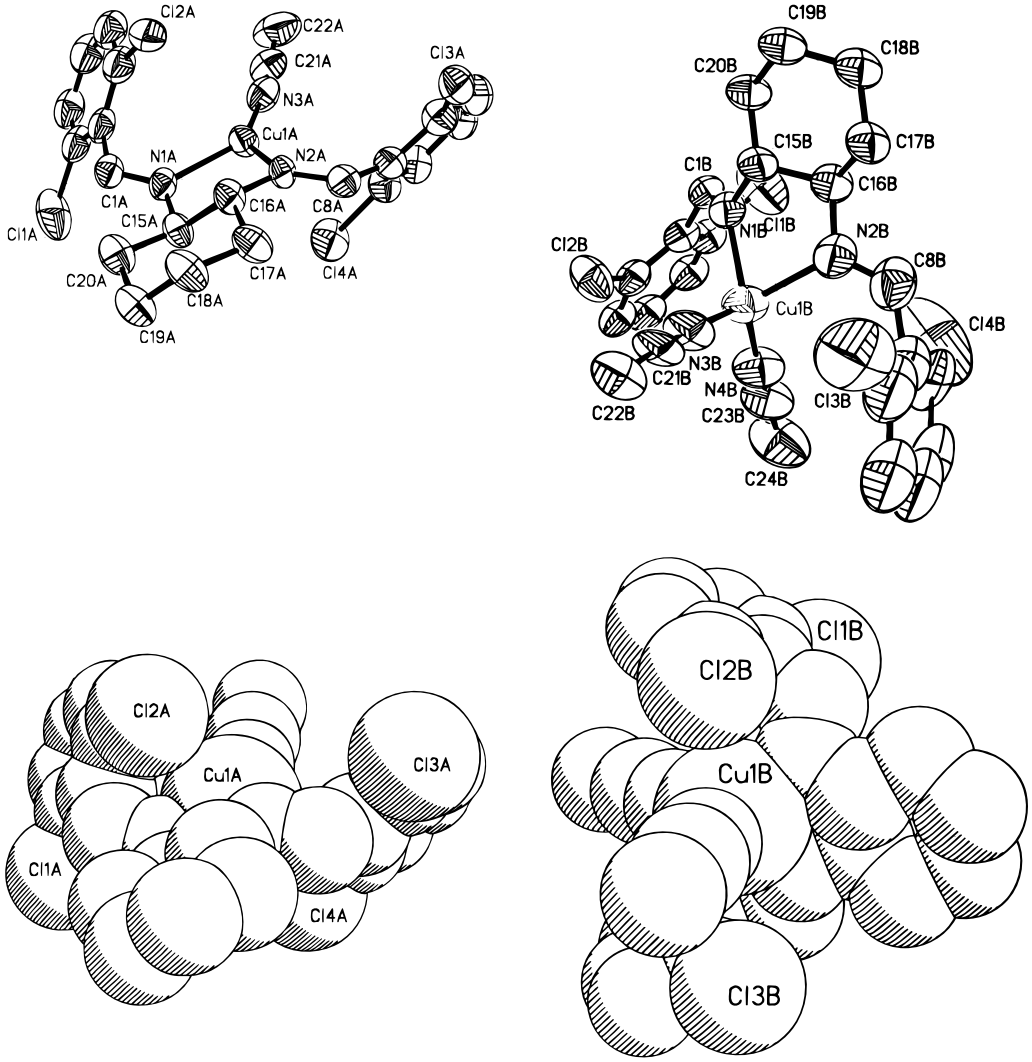

Figure 1. Solid-state structures of the mononuclear components $[Cu^{I}(R,R\text{-}\mathbf{1})(CH_3CN)]^+$ (top left) and $[Cu^{I}(R,R\text{-}\mathbf{1})(CH_3CN)_2]^+$ (top right) in **2**, showing 50% probability ellipsoids and the atom-labeling scheme. Space-filling models of $[Cu^{I}(R,R\text{-}\mathbf{1})(CH_3CN)]^+$ (bottom left) and $[Cu^{I}(R,R\text{-}\mathbf{1})(CH_3CN)_2]^+$ (bottom right) are shown below each structure. Selected interatomic distances (Å) and angles (deg) for $[Cu^{I}(R,R\text{-}\mathbf{1})(CH_3CN)]^+$: Cu1A−N1A 2.077(7), Cu1A−N2A 1.996(6), Cu1A−N3A 1.836(8), N3A−C21A 1.115(10), N3A−Cu1A−N2A 139.6(3), N3A−Cu1A−N1A 136.9(3), N2A−Cu1A−N1A 83.1(3), C1A−N1A−Cu1A 124.1(6), C8A−N2A−Cu1A 126.7(6), N2A−C8A−C9A 121.8(9), N1A−C1A−C2A 122.1(9), N3A−C21A−C22A 176.9(12). For $[Cu^{I}(R,R\text{-}\mathbf{1})(CH_3CN)_2]^+$: Cu1B−N1B 2.111(7), Cu1B−N2B 2.099(8), Cu1B−N3B 1.969(9), Cu1B−N4B 1.914(8), N3B−C21B 1.117(11), N4B−C23B 1.056(10), N4B−Cu1B−N3B 117.8(4), N4B−Cu1B−N2B 111.2(4), N3B−Cu1B−N2B 113.3(3), N4B−Cu1B−N1B 114.6(3), N3B−Cu1B−N1B 114.5(3), N2B−Cu1B−N1B 79.4(3), Cu1B−N2B−C8B 124.6(8), Cu1B−N1B−C1B 133.3(7), N3B−C21B−C22B 177.0(13), N4B−C23B−C24B 179.6(17).

the orifice to skimmer potential ("cone voltage") was varied from 15 to 30 V. Spectra were collected in the multichannel acquisition mode. EI and CI mass spectra were obtained on a Finnigan MAT-90 mass spectrometer. Optical rotations were recorded on a Rudolph Research Autopol III digital polarimeter at 589 nm. Microanalyses were done by H. Kolbe, Mikroanalytisches Laboratorium, Mülheim an der Ruhr, Germany, and by Quantitative Technologies Inc., Whitehouse, NJ.

Results and Discussion

Synthesis and Characterization of Copper(I) Precursor Compounds. Reaction of $[Cu^{I}(MeCN)_4](PF_6)$ (10 mol %) with the chiral Schiff base (1*R*,2*R*)-bis((2,6-dichlorobenzylidene)diamino)cyclohexane (*R*,*R*-**1**, 12 mol %) in CH_2Cl_2 generates a yellow solution which mediates the carbenoid insertion of methyl aryl diazoacetates into the Si−H bond of alkyl and aryl silanes with good to high levels of enantioselection (vide infra). To assess the type of copper compound(s) present in CH_2Cl_2 prior to the addition of any substrate, the yellow solution was concentrated under vacuum and diethyl ether was allowed to diffuse into this solution at −20 °C. Two types of crystalline material are obtained from these solutions. Minor amounts of colorless crystals have been identified by X-ray analysis (see Supporting Information) to be the starting material $[Cu^{I}(CH_3CN)_4](PF_6)\cdot CH_3CN$. The major component of the precipitated material is a yellow crystalline species which has been shown by single-crystal X-ray analysis to consist of three distinct copper-containing sites in a single-crystal lattice, with overall stoichiometry $[Cu^{I}(R,R\text{-}\mathbf{1})(CH_3CN)\cdot Cu^{I}(R,R\text{-}\mathbf{1})(CH_3CN)_2\cdot Cu^{I}_2(R,R\text{-}\mathbf{1})_3](PF_6)_4\cdot 2CH_2Cl_2\cdot 3Et_2O$ (**2**).

Solid-State Structures. The structure of the cationic $[Cu^{I}(R,R\text{-}\mathbf{1})(CH_3CN)]^+$ component in **2** (Figure 1 (top

left)) reveals the presence of a chelating diimino ligand and a single acetonitrile coordinated to a copper ion by virtue of a slightly distorted C_2-symmetric trigonal planar geometry. The deviation from ideal C_2 symmetry is demonstrated by small variations of relevant bond distances (Cu1A−N1A = 2.077(7), Cu1A−N2A = 1.996(6) Å) and angles (N3A−Cu1A−N1A = 136.9(3)°, N3A−Cu1A−N2A = 139.6(3)°, C21A−N3A−Cu1A = 172.5(10)°). As better indicated by the space-filling diagram (Figure 1 (bottom left)), the mutual disposition of the phenyl groups[30] (torsion interplanar angle = 129.9°) is substantially influenced by the presence of the 2,6-dichloro substituents, placing atoms Cl2A and Cl4A in inward positions with respect to the cavity. The copper center lies almost exactly on the imaginary line connecting carbon atoms C2A and C9A of the two phenyl rings (C2A···C9A = 6.5 Å). The cleft generated by the phenyl substituents is anticipated to accommodate the catalytically active carbenoid unit upon displacement of acetonitrile.

The structure of the second mononuclear copper cation in **2**, $[Cu^I(R,R\text{-}\mathbf{1})(CH_3CN)_2]^+$ (Figure 1 (top right)), reveals a distorted tetrahedral metal center (N1B−Cu1B−N2B = 79.3(3)°, N3B−Cu1B−N4B = 117.8(4)°, torsion angle N1B−Cu1B−N2B ∠ N3B−Cu1B−N4B = 89°) which possesses approximate C_2 local symmetry, featuring substantial deviation from ideal C_2 geometry. As the space-filling model indicates (Figure 1 (bottom right)), the two flanking phenyl groups are positioned in a manner similar to that observed in the case of the trigonal-planar copper complex. The cavity so generated is occupied by two acetonitrile moieties oriented at positions of minimum interaction in relation to the phenyl groups. In contrast to the trigonal-planar copper site, the tetrahedrally coordinated copper(I) is coordinatively and electronically saturated and would thus require dissociation of at least one acetonitrile prior to coordination of any substrate moiety.

The structure of the unique dicopper species $[Cu^I{}_2(R,R\text{-}\mathbf{1})_3]^{2+}$ in **2** (Figure 2 (top)) reveals two trigonal-planar copper centers, each coordinated by a chelating diimine ligand and connected to the other copper site via a third diimine ligand that acts as bridging rather than chelating moiety. An approximate local C_2 axis passes through the bridging diimino ligand, bisecting internuclear distances C15−C16 and C18−C19. The mutual orientation of the flanking phenyl groups of the chelating diimino ligands defines a substantially wider cavity than that observed in the case of the mononuclear sites, reflecting the flexibility of the chelating diimino ligand to accommodate a moiety in the cleft that is more sterically demanding than acetonitrile. In the cavity, the pendant phenyl and cyclohexane units associated with the bridging diimine ligand assume a configuration of minimum interaction vis-à-vis the phenyl groups of the chelating diimine ligands. The mode of coordination displayed by the bridging diimino unit exemplifies the potential of the present ligand to effect undesirable oligomerization of chiral copper centers[31] at a ligand-to-copper ratio of ≥1. Space-filling models of the dicopper complex (Figure 2 (bottom)) indicate that each copper ion is tightly protected from substrate binding by the surrounding dichloro-substituted phenyl groups and central cyclohexane ring. The position of the pendant phenyl and cyclohexane units associated with the bridging diimine ligand is indicative of the orientation expected of the docking carbene moiety upon catalysis.

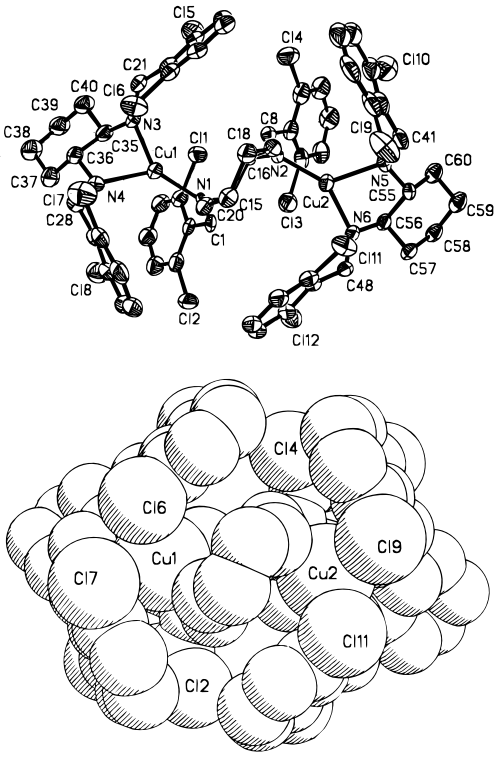

Figure 2. Solid-state structure of the dinuclear species $[Cu^I{}_2(R,R\text{-}\mathbf{1})_3]^{2+}$ (top) in **2**, showing 50% probability ellipsoids and the atom-labeling scheme, and space-filling model (bottom). Selected interatomic distances (Å) and angles (deg): Cu1−N1 1.911(6), Cu1−N3 2.032(6), Cu1−N4 2.048(6), Cu2−N2 1.941(6), Cu2−N6 2.025(6), Cu2−N5 2.073(6), N1−Cu1−N3 141.9(2), N1−Cu1−N4 135.1(2), N3−Cu1−N4 80.8(2), N2−Cu2−N5 131.3(2), N2−Cu2−N6 144.1(2), N6−Cu2−N5 82.5(2), Cu1−N3−C21 138.1(6), Cu1−N4−C28 128.1(6), Cu1−N1−C1 124.0(6), Cu2−N2−C8 121.9(6), Cu2−N5−C41 126.9(6), Cu2−N6−C48 135.2(6).

Solution Structures. To examine which of the above species, and possibly others, are present in solution at concentrations pertaining to catalytic conditions, a spectroscopic examination of the system $[Cu^I(MeCN)_4](PF_6)$ (3.20×10^{-5} M)/*R*,*R*-**1** (3.84×10^{-5} M) was undertaken in CH_2Cl_2. The ^{1}H NMR spectrum of this catalytic combination in CD_2Cl_2 at 25 °C shows the presence of only one set of well-resolved ligand-based protons and a sharp resonance due to CH_3CN. No appreciable broadening or further resolution of these resonances is observed at lower temperatures (from 25 to −80 °C), indicating the presence of a single major copper species in solution. However, careful inspection of the ^{1}H NMR spectrum's baseline suggests that residual weak resonances may be due to other ligated copper species present in minor amounts (≤5%).

(30) For selectivity imposed by aromatic interactions in substrate binding see: (a) Quan, R. W.; Jacobsen, E. N. *J. Am. Chem. Soc.* **1996**, *118*, 8156−8157. (b) Evans, D. A.; Kozlowski, M. C.; Murry, J. A.; Burgey, C. S.; Campos, K. R.; Connell, B. T.; Staples, R. J. *J. Am. Chem. Soc.* **1999**, *121*, 669−685.

(31) For similar formation of chiral Cu(I) polymers see: Evans, D. A.; Woerpel, K. A.; Scott, M. J. *Angew. Chem., Int. Ed. Engl.* **1992**, *31*, 430−432.

To further investigate the identity of the ^{1}H NMR active species and other low-concentration copper-containing components, positive-ion electrospray ionization mass spectrometry (ESI-MS) was applied to yellow solutions of $[Cu^I(CH_3CN)_4](PF_6)$/*R,R*-**1** in CH_2Cl_2 at concentrations noted above. At low cone voltages, the major molecular ion revealed by ESI-MS possesses the correct mass (m/z = 532 amu) and isotopic distribution for $[Cu^I(R,R\text{-}\mathbf{1})(CH_3CN)]^+$ and is accompanied by its acetonitrile-free fragment $[Cu^I(R,R\text{-}\mathbf{1})]^+$ (m/z = 491 amu), the latter increasing in abundance with increasing cone voltage at the expense of $[Cu^I(R,R\text{-}\mathbf{1})(CH_3CN)]^+$. A second low-abundance ion evident in the ESI-MS spectrum, but surprisingly not encountered among the solid-state counterparts, corresponds in mass (m/z = 919 amu) and isotopic distribution to $[Cu^I(R,R\text{-}\mathbf{1})_2]^+$. Varying the ratio of $[Cu^I(CH_3CN)_4](PF_6)$/(R,R-**1**) from 0.8 to 1.2 results in similar ESI-MS spectra, with the exception that at the higher end of the range $[Cu^I(R,R\text{-}\mathbf{1})_2]^+$ is almost completely suppressed in favor of the ion $[Cu^I(CH_3CN)_2]^+$ (m/z = 145 amu), a fragment of $[Cu^I(CH_3CN)_4]^+$. Otherwise, the crystallographically documented ions $[Cu^I(R,R\text{-}\mathbf{1})(CH_3CN)_2]^+$ and $[Cu^I_2(R,R\text{-}\mathbf{1})_3]^+$ are present only in trace amounts. It is conceivable that the representation of these ions in isolable amounts in the solid state is favored by equilibria influenced by the crystallization procedure.

We conclude then that $[Cu^I(R,R\text{-}\mathbf{1})(CH_3CN)]^+$ is the major (>95%) copper-containing species in solutions of $[Cu^I(CH_3CN)_4](PF_6)$ and R,R-**1** in CH_2Cl_2 at concentrations pertinent to catalysis. Other detectable copper complexes, with most prominent the $[Cu^I(R,R\text{-}\mathbf{1})_2]^+$ and $[Cu^I(CH_3CN)_4]^+$ ions, are present in minor or trace amounts ($[Cu^I(R,R\text{-}\mathbf{1})(CH_3CN)_2]^+$, $[Cu^I_2(R,R\text{-}\mathbf{1})_3]^+$).

Stoichiometric Reactions of the $[Cu^I(CH_3CN)_4](PF_6)$/*R,R*-1 System. (a) Aryl Diazoesters. To assess the order by which the active copper site(s) may activate the two substrates of the carbenoid Si−H insertion reaction, and possibly gain insight into the intermediates generated, we performed stoichiometric reactions of $[Cu^I(CH_3CN)_4](PF_6)$/R,R-**1** with aryl diazoesters and silanes, conducted separately for each substrate.

The reaction of $[Cu^I(CH_3CN)_4](PF_6)$ (10%) and R,R-**1** (12%) with 1 equiv of $PhC(N_2)CO_2Me$ in CH_2Cl_2 was followed by variable-temperature ^{1}H NMR, UV−vis, and ESI-MS spectroscopies. Apparently, no reaction takes place in the temperature range from −80 to −15 °C for a period of 1 h, but within the temperature window from −10 to 0 °C, a rapid change of color occurs from an initial yellow to a deep red-orange solution (λ_{max} = 277, 298 (br), 429 (br) nm). ^{1}H NMR spectra indicate that in the temperature region above −10 °C $PhC(N_2)CO_2Me$ (conveniently followed by observing the proton resonance of CO_2CH_3 at δ = 3.83) is progressively consumed, while three thermally stable products emerge which incorporate the carbenoid moiety (δ = 3.99, 3.79, and 3.53 (CO_2CH_3)). Following chromatographic purification, these products have been identified by ^{1}H NMR and HRMS, and by comparison with authentic samples, to be $PhCOCO_2Me$ (δ = 3.99 (minor product)) and *cis*/*trans*-$PhC(CO_2Me)$=$CPh(CO_2Me)$ (major products). Despite the appearance of several minor resonances that can be partly due to the colored species, no positive identification of this thermally unstable intermediate could be made by ^{1}H NMR, probably owing to its low concentration in solution. As evidenced by ^{1}H NMR, the major copper-containing species in these solutions is still the $[Cu^I(R,R\text{-}\mathbf{1})(CH_3CN)]^+$ ion.

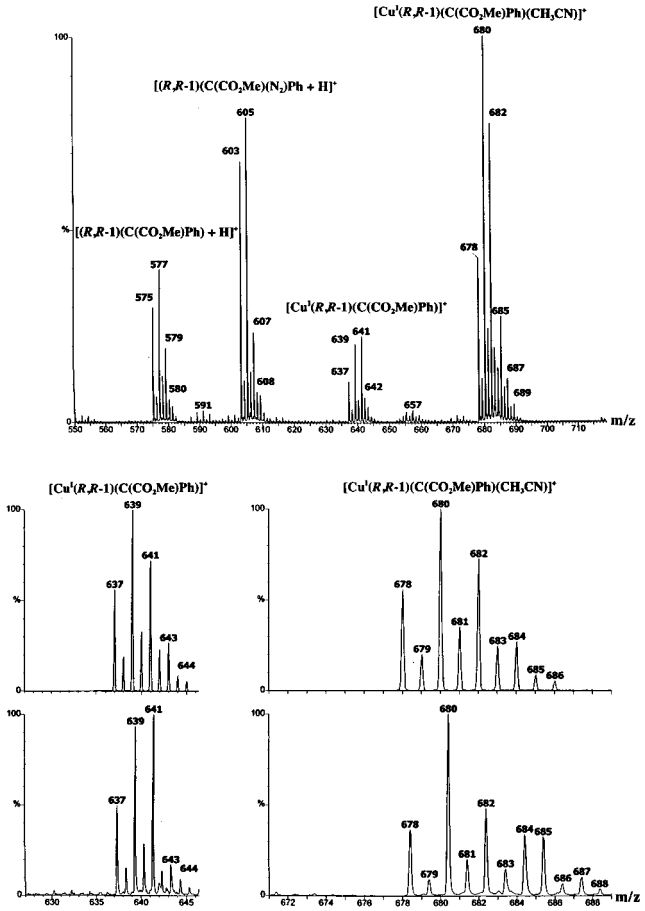

Figure 3. (Top) Positive-ion electrospray ionization MS spectrum of solutions of $[Cu(CH_3CN)_4](PF_6)$/R,R-**1** and $PhC(N_2)CO_2Me$ in CH_2Cl_2. (Bottom) Theoretical (above) and experimental (below) ESI-MS spectra of $[Cu^I(R,R\text{-}\mathbf{1})(C(CO_2Me)Ph)]^+$ (left) and $[Cu^I(R,R\text{-}\mathbf{1})(C(CO_2Me)Ph)(CH_3CN)]^+$ (right).

Positive-ion electrospray ionization MS (ESI-MS) was then employed to identify molecular ions at low concentrations. Addition of 0.3 equiv of $PhC(N_2)CO_2Me$ to $[Cu^I(CH_3CN)_4](PF_6)$/R,R-**1** (1:1.2) in ice-cold CH_2Cl_2 generates a red-orange solution, which upon examination by ESI-MS (cone voltage 5−30 V) gives rise to four novel low-yield molecular ions (Figure 3 (top)), in addition to those observed by ESI-MS in solutions of $[Cu^I(CH_3CN)_4](PF_6)$/R,R-**1** alone, as noted above. Two of these ions contain copper and have been assigned by mass and isotopic distribution to $[Cu^I(R,R\text{-}\mathbf{1})(C(CO_2Me)Ph)]^+$ (m/z = 639 amu) and $[Cu^I(R,R\text{-}\mathbf{1})(C(CO_2Me)Ph)(CH_3CN)]^+$ (m/z = 680 amu) (Figure 3 (bottom)). The other two ions are devoid of copper and correspond to $[(R,R\text{-}\mathbf{1})(C(CO_2Me)Ph) + H]^+$ (m/z = 577 amu) and $[(R,R\text{-}\mathbf{1})(C(CO_2Me)(N_2)Ph + H]^+$ (m/z = 605 amu). The observed ions $[Cu^I(R,R\text{-}\mathbf{1})(C(CO_2Me)Ph]^+$ and $[Cu^I(R,R\text{-}\mathbf{1})(C(CO_2Me)Ph)(CH_3CN)]^+$ are consistent with the presence of the carbenoid unit Cu=$C(CO_2Me)Ph$, although bond connectivities cannot be established. Dinitrogen adducts of these copper-containing species are not detected even at very low cone voltages; thus it is

unlikely that the observed ions are fragments of their diazo precursors. Apparently, acetonitrile can coordinate to copper simultaneously with the carbenoid unit. It is unlikely that MeCN is solvated rather than metal coordinated, as the ion persists undiminished even at high cone voltages. It is presently unclear whether any of these copper-containing ions are also responsible for the observed transient red-orange color. We note however that the absorption shifts to purple in the case of the para-substituted phenyl diazoester *p*-MeO-PhC-$(N_2)CO_2Me$.

(b) Silanes. An important manifestation of the catalytic reaction is that a small amount of an orange-brownish flocculent material is generated at room temperature upon stirring the solution of the organosilane and $[Cu^I(MeCN)_4](PF_6)$/*R*,*R*-**1** for 5 min prior to adding the diazoester. To gain better understanding of this unanticipated reaction, $[Cu^I(MeCN)_4](PF_6)$/*R*,*R*-**1** was mixed with 1 equiv of $PhMe_2Si$-H in CD_2Cl_2, stirred for an hour, and centrifuged, and the supernatant was examined by ^1H NMR, using hexamethylbenzene as internal standard. These ^1H NMR spectra indicate that all starting components of the mixture are retained almost at the initial levels, apparently without any detectable new features, suggesting that the observed interaction is a low-yield event. Surprisingly, the flocculent precipitant can be resuspended in CH_2Cl_2 to generate a mixture which can still mediate the insertion of $PhC(N_2)CO_2Me$ into the Si−H bond of $PhMe_2Si$-H, albeit at low yield (<10%) and selectivity (10% ee). The supernatant is also catalytically active, providing comparable levels of stereocontrol versus the corresponding catalytic reaction in which the precipitant has not been centrifuged off. As aryl silanes are known to be good hydride donors,[32] these results raise suspicions whether any copper hydride species formed in minute amounts are participating in the catalytic cycle (vide infra).

(c) Other Small Molecules. To assess the electron donor ability of the copper site toward stabilizing the carbenoid moiety, the electronically similar CO was allowed to react with yellow solutions of $[Cu^I(MeCN)_4](PF_6)$/*R*,*R*-**1** in CH_2Cl_2. The solution turned pale yellow, and colorless crystals of $[Cu^I(R,R\text{-}\mathbf{1})(CO)](PF_6)$, not suitable for X-ray analysis, were deposited upon diffusion of diethyl ether. The diagnostic ν_{CO} stretching frequency at 2092 cm^{-1} indicates that the degree of Cu−CO stabilization due to π-back-bonding is limited, as expected for late transition elements. Apparently, the Cu−CO bond is loosely held together owing to its σ-bonding component or, as recently suggested,[33] due to a predominant electrostatic interaction operating in this type of late transition metal cationic species. The weakness of the Cu−CO interaction is also indicated by the reversibility of the CO addition reaction under vacuum or a stream of argon. The modest π-back-donation is expected to be beneficial to the catalytic properties of the copper carbenoid moiety, inasmuch as the electrophilic nature of the metal bound carbene will be preserved, and the electron density associated with the Cu−C bond will be readily available for the Si−H insertion process.

Table 2. Catalytic Insertion of Methyl Phenyldiazoester into Si−H Bonds of Silanes

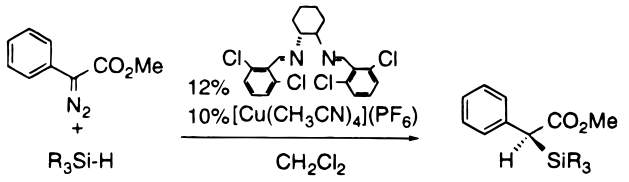

silane	cone angle[a] (deg)	χ^b	*T* (°C)	yield (%)	*S*/*R*	ee (%)
$PhMe_2SiH$	122	10.60	0	88	7.61	76
$PhMe_2SiH$	122	10.60	−40	85	10.77	83
Ph_2MeSiH	136	12.10	0	79	6.70	74
Ph_2MeSiH	136	12.10	−40	77	11.00	84
Ph_3SiH	145	13.25	0	87	2.89	49
Ph_3SiH	145	13.25	−40	47	6.07	72
Et_3SiH	132	6.30	0	90	6.99	75
Et_3SiH	132	6.30	−40	87	10.51	83
$(n\text{-}Bu)_3SiH$	136	5.25	0	83	9.87	82
$(n\text{-}Bu)_3SiH$	136	5.25	−40	84	15.44	88
$(n\text{-}Hex)_3SiH$	136	5.00	0	87	10.77	83
$(n\text{-}Hex)_3SiH$	136	5.00	−40	73	12.70	87
$(i\text{-}Pr)_3SiH$	160	3.45	0	71	3.64	57
$(i\text{-}Pr)_3SiH$	160	3.45	−40	NR[c]	N/A	N/A
$(i\text{-}Bu)_3SiH$	143	5.70	0	94	9.95	82
$(i\text{-}Bu)_3SiH$	143	5.70	−40	NR	N/A	N/A
$(Me_3Si)_3SiH$	182	0.80	0	45	9.98	84
$(Me_3Si)_3SiH$	182	0.80	−40	NR	N/A	N/A
$(t\text{-}Bu)_2MeSiH$	161	2.85	−10	80	9.00	80
$(t\text{-}Bu)_2MeSiH$	161	2.85	−40	NR	N/A	N/A

[a] Tolman's cone angles.[41] [b] Electronic parameter χ.[42] [c] NR = no reaction.

Attempts to gain insight into the geometric features and interactions of the Cu−C(CO_2Me)Ph unit within the ligand cavity, by means of installing a mimicking Cu−S(CO_2Et)Ph moiety, were not successful. Crystals obtained by diffusion of diethyl ether into a solution of $[Cu^I(MeCN)_4](PF_6)$/*R*,*R*-**1** and $PhSCO_2Et$ in CH_2Cl_2 were shown by X-ray analysis (see Supporting Information) to be $[Cu^I_2(R,R\text{-}\mathbf{1})_3](PF_6)_2 \cdot PhSCO_2Et \cdot 0.75CH_2Cl_2 \cdot 0.5CH_3CN$. The molecule features the same dinuclear copper unit found in **2**, and $PhSCO_2Et$ appears to be solvated in the crystal lattice rather than coordinated to the copper site.

Catalytic Carbenoid Si−H Insertion Reactions. Yellow solutions of $[Cu^I(MeCN)_4](PF_6)$ (10 mol %) and *R*,*R*-**1** (12 mol %) in CH_2Cl_2 mediate carbenoid insertion of methyl phenyl diazoacetate to the Si−H bond of organosilanes with good to high yields and levels of enantiocontrol[34] (Table 2). The absolute stereochemistry of the major enantiomer obtained from the *R*,*R*-**1** ligand has been determined to be (*S*) by virtue of its transformation to the corresponding methyl-(*S*)-(+)-mandelate.[35] The catalytic reactions are performed in the temperature range between 0 and −40 °C, since carbenoid Si−H inserion reactions conducted below −40 °C proved to be impractically slow, whereas at temperatures above 0 °C the level of enantiocontrol is seriously compromised. Moreover, use of $[Cu^I_2(C_6H_6)(OTf)_2]$[36] rather than $[Cu^I(MeCN)_4](PF_6)$ provides comparable

(32) Hays, D. S.; Fu, G. C. *J. Org. Chem.* **1997**, *62*, 7070−7071.
(33) Goldman, A. S.; Krogh-Jespersen, K. *J. Am. Chem. Soc.* **1996**, *118*, 12159−12166.
(34) For reviews on the synthetic scope of chiral silane reagents see: (a) Fleming, I.; Barbero, A.; Walter, D. *Chem. Rev.* **1997**, *97*, 2063-2192. (b) Masse, C. E.; Panek, J. S. *Chem. Rev.* **1995**, *95*, 1293−1316.
(35) Fleming, I. *Chemtracts Org. Chem.* **1996**, *9*, 1−64.
(36) Salomon, R. G.; Kochi, J. K. *J. Am. Chem. Soc.* **1973**, *95*, 3300−3310.

results in terms of yield and enantioselectivity, but the air-sensitivity of the reagent makes its use less convenient. In contrast, $[Cu^{II}(OTf)_2]$ markedly diminishes the levels of enantiocontrol.[37] Importantly, $[Cu^{I}(MeCN)_4](PF_6)$ (10 mol %) alone mediates carbenoid Si−H insertion, as evidenced by the formation of the racemic mixture of products derived from the carbenoid insertion of $PhC(N_2)CO_2Me$ into $PhMe_2Si$-H. The reaction is faster than the corresponding reaction in the presence of ligand, as indicated by monitoring the product yields of the ligand-free reaction (83% at 0 °C, 2 h) versus those of the reaction in the presence of ligand (69%). However, the final yield drops to less than 5% if the concentration of $[Cu^{I}(MeCN)_4](PF_6)$ is diminished to 1 mol %. Apparently, the frequently observed "ligand acceleration" phenomenon[38] is not operative in the present instance. It is also notable that the ligand *R*,*R*-**1** has been selected among a wide range of other aryl-substituted diimine ligands (aryl = phenyl, 1-naphthyl, 2,6-$F_2C_6H_3$, 4-ClC_6H_4, 2,4,6-$Me_3C_6H_2$, 3,5-$(CF_3)_2C_6H_3$, 2,5,6-$Cl_3C_6H_2$) and is remarkably the same as that which induces the highest levels of enantioselectivity in cyclopropanation and aziridination reactions.[14,15] Moreover, the presence of the aryl substituent on the carbenoid precursor has proven to be essential in imparting high levels of enantiocontrol. For instance, the vinyl diazoesters $RCH{=}CH(N_2)CO_2Me$ (R = Me, Et, Ph) insert into the Si−H bond of $PhMe_2Si$-H with very low selectivities (ee = 17−36%).

Mechanistic Investigations. (a) Linearity of Correlation between ee of Product and ee of Ligand. The presence of potentially active copper sites in which more than one exchangeable chiral ligand is coordinated per copper ion or cluster (as for instance in $[CuL_2]^+$ or $[Cu_2L_3]^{2+}$) can lead, according to Kagan's analysis,[39] to nonlinear correlations[40] between the ee of the product and the ee of the ligand (or auxiliary). Taking active $[CuL_2]^+$ ions as an example and assuming that enantiomerically impure ligand is employed (for instance if L is a mixture of *R*,*R*-**1** and *S*,*S*-**1**), nonlinear effects would arise due to the presence of active or inactive meso species $[Cu(R,R\text{-}\mathbf{1})(S,S\text{-}\mathbf{1})]^+$. The sole exception leading to linearity is the remote case of equal reactivity between the meso species and its homochiral congeners, yielding racemic and enantiomeric products, respectively. Otherwise, "positive" deviation from linear correlation between ee of the product and ee of the ligand is expected if the reactivity of the meso species is inferior to that of the homochiral catalysts (maximum deviation is achieved in the event of an inactive meso species) and "negative" deviation in the reverse scenario. Presumably, "negative" nonlinear behavior can also be obtained due to the presence of metal species (in the present case $[Cu^{I}(MeCN)_4]^+$) which remain uncomplexed by the chiral ligand and mediate the formation of racemic product at rates superior to those associated with the production of the enantiomerically enriched product. An additional source of nonlinear behavior discussed by Kagan[39] consists of accumulation of catalytically inactive metal reagents (usually products of polymerization) complexed by chiral ligands that feature an overall ee value that deviates from the nominal ee value of the initially added ligand. Nonlinear correlation of ee of the product versus the ee of the ligand would then arise because the remaining pool of catalytically active metal sites retains ligands with an "effective" ee that also differs from the nominal ee value.

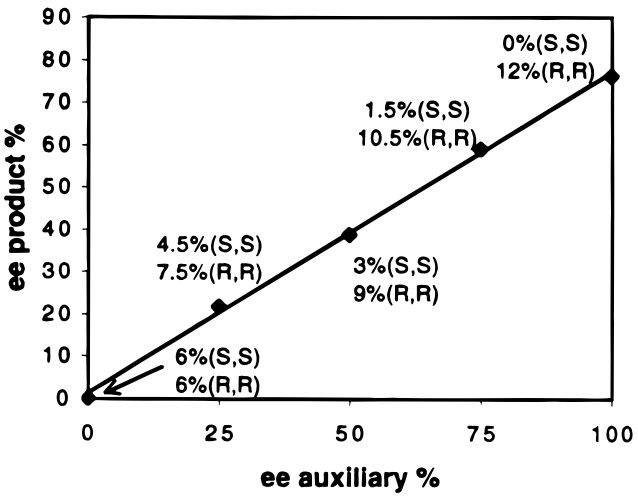

Figure 4. Correlation of the enantioselectivity of carbenoid $PhC(N_2)CO_2Me$ insertion into the Si−H bond of $PhMe_2Si$-H as a function of the enantioselectivity of ligand **1** varied as noted in the figure. The catalyst is $[Cu(CH_3CN)_4](PF_6)$ (10%)/**1** (12%) in CH_2Cl_2 at 0 °C.

The linearity test is used in the present study as a mechanistic criterion of the importance of copper-containing species other than the mononuclear $[(R,R\text{-}\mathbf{1})Cu(CH_3CN)_n]^+$ ions in interfering with the outcome of enantioselection. Those include ions that have been structurally identified in the solid state and/or in solution ($[Cu(CH_3CN)_4]^+$, $[Cu_2(R,R\text{-}\mathbf{1})_3]^{2+}$, $[Cu(R,R\text{-}\mathbf{1})_2]^+$). Figure 4 indicates that, for a series of $[Cu^{I}(MeCN)_4](PF_6)$/**1** reagents for which the ee of **1** was intentionally varied from 0 to 100% by mixing appropriate amounts of *R*,*R*-**1** and *S*,*S*-**1**, the ee of the product of $PhC(N_2)CO_2Me$ insertion into $PhMe_2Si$-H correlates in a perfectly linear fashion ($R^2 = 0.998$) with the ee of the ligand. This result is consistent with the exclusive operation of mononuclear $[Cu(\mathbf{1})]^+$-type units in solution and diminishes the importance of any other copper-containing species in conferring mechanistic complexity. Presumably, these peripheral copper sites are present in minute amounts and/or are unproductive and in any event do not alter the enantiomeric integrity of the ligand or product associated with or generated by the catalytically active copper centers. A linear correlation between ee of the product and ee of the ligand has been previously reported[14] for asymmetric cyclopropanation and aziridination reactions catalyzed by the present Cu(I) diimine reagents.

(b) Stereoelectronic Effects. Linear Free-Energy Relationships. Inspection of the ee values for a series of aryl and alkyl silanes (Table 2) reveals that the levels

(37) Carbenoid Si−H insertion reactions mediated by achiral Cu(II) reagents have been previously demonstrated: (a) Bagheri, V.; Doyle, M. P.; Taunton, J.; Claxton, E. E. *J. Org. Chem.* **1988**, *53*, 6158−6160. (b) Andrey, O.; Landais, Y.; Planchenault, D.; Weber, V. *Tetrahedron* **1995**, *51*, 12083−12096.

(38) (a) Jacobsen, E. N.; Markó, I.; Mungall, W. S.; Schröder, G.; Sharpless, K. B. *J. Am. Chem. Soc.* **1988**, *110*, 1968−1970. (b) Jacobsen, E. N.; Markó, I.; France, M. B.; Svendsen, J. S.; Sharpless, K. B. *J. Am. Chem. Soc.* **1989**, *111*, 737−739.

(39) Guillaneux, D.; Zhao, S.-H.; Samuel, O.; Rainford, D.; Kagan, H. B. *J. Am. Chem. Soc.* **1994**, *116*, 9430−9439.

(40) Puchot, C.; Samuel, O.; Duñach, E.; Zhao, S.; Agami, C.; Kagan, H. B. *J. Am. Chem. Soc.* **1986**, *108*, 2353−2357.

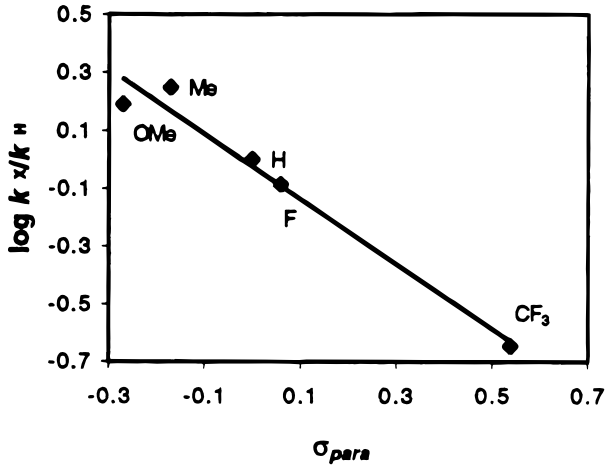

Figure 5. Correlation of the reactivity of carbenoid *p*-X-PhC(N_2)CO_2Me insertion into the Si−H bond of $PhMe_2$Si-H as a function of σ_{para} values of the substituent X. The reactivity is expressed as log of the ratio of carbenoid insertion products of *p*-X-PhC(N_2)CO_2Me over PhC(N_2)CO_2Me.

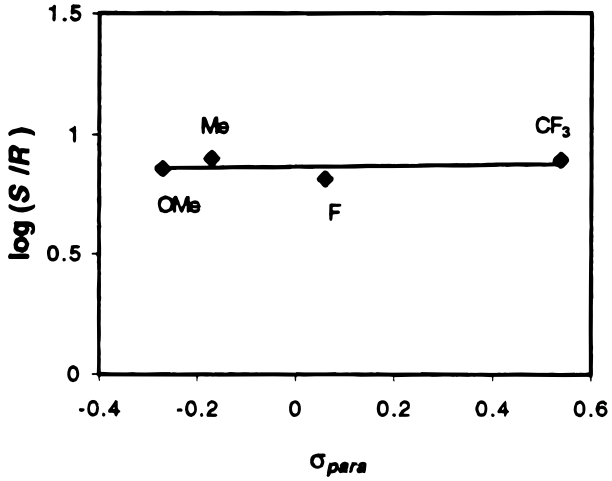

Figure 6. Correlation of the enantioselectivity of carbenoid *p*-X-PhC(N_2)CO_2Me insertion into the Si−H bond of $PhMe_2$Si-H as a function of σ_{para} values of the substituent X. The enantioselectivity is expressed as log of the ratio of the carbenoid insertion enantiomers (major over minor).

of enantiocontrol are largely insensitive to the steric and electronic properties of the silanes, inasmuch as the ee values vary in a narrow range (72−88%) for silanes exhibiting wide distribution of Tolman's cone angles[41] and electronic χ parameters.[42] Two notable exceptions are encountered with the silanes Ph_3Si-H and (i-Pr)$_3$Si-H, for which the corresponding ee values (49 and 57%, respectively) at 0 °C are markedly low. The low yields obtained in the case of the good hydride donor (Me_3Si)$_3$SiH[43] are associated with high yields of isolable $PhCH_2CO_2Me$.

To closely investigate the electronic properties of the transition state for the carbenoid Si−H insertion reaction, a series of para-substituted aryl methyl diazoacetates (*p*-X-PhC(N_2)CO_2Me; X = MeO, Me, H, F, CF_3) has been employed. A Hammett plot (Figure 5) of log(k_X/k_H) as a function of the characteristic σ_{para} value for each substituent affords a satisfactory linear correlation ($\rho = -1.12$, $R^2 = 0.970$), suggesting the presence of a sizable positive charge on the carbenoid carbon in the transition state. The ratio k_X/k_H is determined by measuring relative product yields, assuming that the reaction is under kinetic control. Surprisingly, the corresponding plot (Figure 6) of log of the ratio of enantiomers (*S*(major)/*R*(minor)) as a function of σ_{para} indicates that the levels of enantiocontrol are insensitive to the electronic properties of the carbenoid intermediate.

The electronic properties of the transition state, as influenced by the silane component, have also been evaluated with the aid of a series of para-substituted aryl silanes (*p*-X-$PhMe_2$Si-H; X = MeO, Me, H, F, CF_3). A Hammett plot (Figure 7) of log(k_X/k_H) (derived by competition kinetics) as a function of σ_{para} features a reasonably linear relationship ($\rho = -0.54$, $R^2 = 0.960$), suggesting that a small partial positive charge resides on the silicon atom as part of the transition state. However, the corresponding diagram (Figure 8) of the

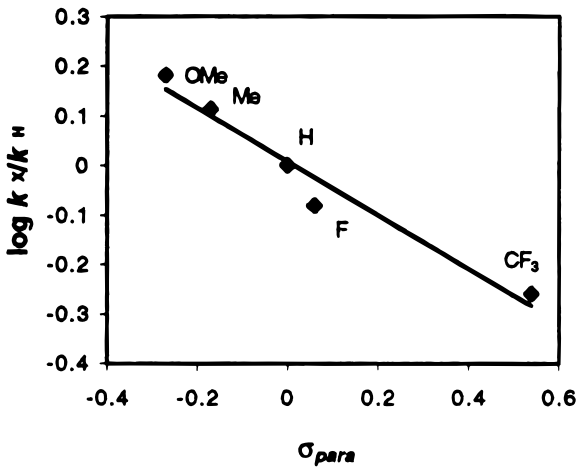

Figure 7. Correlation of the reactivity of carbenoid PhC-(N_2)CO_2Me insertion into the Si−H bond of *p*-X-$PhMe_2$Si-H as a function of σ_{para} values of the substituent X. The reactivity is expressed as log of the ratio of carbenoid insertion products of *p*-X-$PhMe_2$Si-H over $PhMe_2$Si-H.

log of the ratio of enantiomers (*S*(major)/*R*(minor)) as a function of σ_{para} reveals no correlation between the electronic properties of the silane and the enantioselectivity of the carbenoid insertion reaction into the Si−H bond. Taken together, these Hammett correlations suggest that stabilization of the positive charge developed on both the carbon atom of the carbenoid and the silicon atom of the silane enhances the reactivity but apparently does not influence the selectivity of the process.

(c) Temperature Dependence of Enantioselectivity. To investigate whether the observed enantioselectivity may be determined in a stepwise mechanism (for instance, in two selection steps[44] which may become

(41) Tolman, C. A. *Chem. Rev.* **1977**, *77*, 313−348.
(42) Bartik, T.; Himmler, T.; Schulte, H.-G.; Seevogel, K. *J. Organomet. Chem.* **1984**, *272*, 29−41.
(43) (a) Chatgilialoglu, C. *Chem. Rev.* **1995**, *95*, 1229−1251. (b) Chatgilialoglu, C. *Acc. Chem. Res.* **1992**, *25*, 188−194.
(44) (a) Haag, D.; Runsink, J.; Scharf, H.-D. *Organometallics* **1998**, *17*, 398−409. (b) Enders, D.; Gielen, H.; Breuer, K. *Tetrahedron: Asymmetry* **1997**, *8*, 3571−3574. (c) Heller, D.; Buschmann, H.; Scharf, H.-D. *Angew. Chem., Int. Ed. Engl.* **1996**, *35*, 1852−1854. (d) Göbel, T.; Sharpless, K. B. *Angew. Chem., Int. Ed. Engl.* **1993**, *32*, 1329−1331.

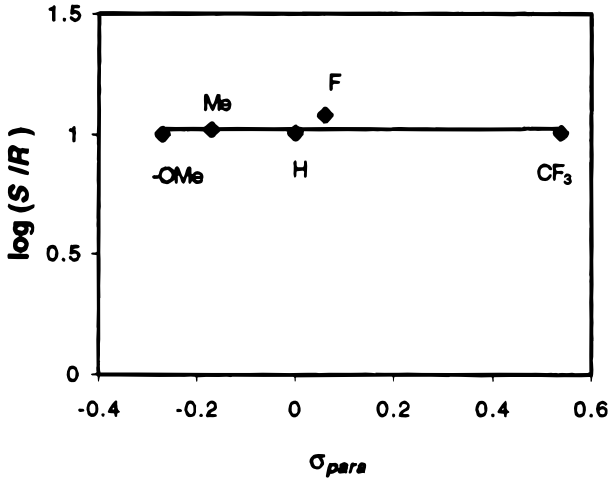

Figure 8. Correlation of the enantioselectivity of carbenoid $PhC(N_2)CO_2Me$ insertion into the Si−H bond of *p*-X-$PhMe_2Si$-H as a function of σ_{para} values of the substituent X. The enantioselectivity is expressed as log of the ratio of the carbenoid insertion enantiomers (major over minor).

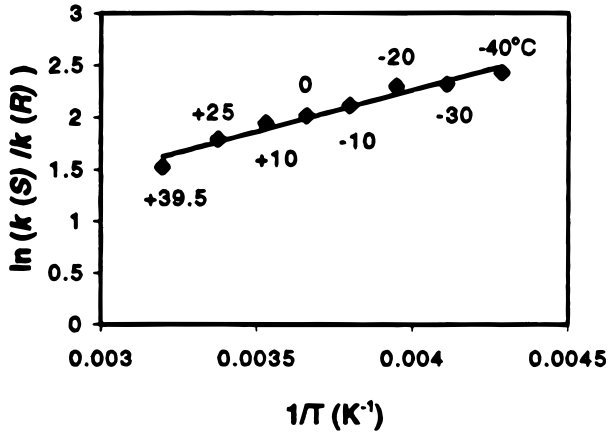

Figure 9. Eyring plot for the carbenoid $PhC(N_2)CO_2Me$ insertion into the Si−H bond of $PhMe_2Si$-H mediated by $[Cu(CH_3CN)_4](PF_6)$ (10%)/*R*,*R*-**1** (12%) in CH_2Cl_2.

rate limiting in different temperature regions (Scarf behavior[45])), we examined the temperature dependence of enantiopurity according to the modified Eyring equation:[46]

$$\ln P = -\Delta\Delta H^{\ddagger}/RT + (\Delta\Delta S^{\ddagger}/R) \qquad (8)$$

where *P* is the ratio of overall rate constants *k*(major enantiomer)/*k*(minor enantiomer). For the $[Cu^{I}(MeCN)_4](PF_6)$/*R*,*R*-**1**-mediated insertion of the carbenoid precursor $PhC(N_2)CO_2Me$ into the Si−H bond of $PhMe_2Si$-H, an Eyring plot (Figure 9) of ln(*k*(*S*)/*k*(*R*)) (calculated from the ratio of amounts of major (*S*) over minor (*R*) enantiomer, assuming kinetic control in the formation of products) as a function of 1/*T* over the temperature range from −40 to +40 °C reveals a satisfactory linear relationship ($R^2 = 0.960$), although excellent nonlinear fits to polynomial expressions can also be obtained. The lack of an apparent inversion temperature which separates two linear regions, as evidenced in numerous other cases of chemoselective systems,[44] argues that determination of enantioselectivity in a single step cannot be excluded with the present system. Ridd's analysis[46b] of certain combinations of activation parameters that would afford linear plots of ln *P* versus 1/*T* in two-step selection processes exemplifies the limitations of taking the linearity of these plots as a strict mechanistic criterion. However, if a one-step selection level is truly operative, then the activation parameters $\Delta\Delta H^{\ddagger}$ and $\Delta\Delta S^{\ddagger}$ derived from the modified Eyring plot are meaningful. The values calculated from the slope and intercept of Figure 9 ($\Delta\Delta H^{\ddagger} = -1.58 \pm 0.13$ kcal mol^{-1}; $\Delta\Delta S^{\ddagger} = -1.82 \pm 0.49$ cal mol^{-1} K^{-1}) indicate that the energetic difference in the diastereotopic transition states is subject to not only enthalpic but also significant entropic discrimination. The latter may be better understood in terms of an early, less structured, transition state.[47]

(d) Determination of the Primary Deuterium Kinetic Isotope Effect (KIE) and Its Temperature Dependence. To evaluate the involvement of carbenoid Si−H insertion in the rate-limiting step and possibly assess the relative geometry and position of the transition state with respect to Si−H bond activation, a primary KIE has been determined by allowing intermolecular competition for carbenoid Si−H(D) insertion into $PhMe_2Si$-H/$PhMe_2Si$-D (1:1) at 0 °C. The value so obtained ($k_H/k_D = 1.29$) is relatively small but significant. In addition, the k_H/k_D value varies significantly with temperature (from 2.12 (−40 °C) to 1.08 (25 °C) (vide infra)), suggesting that Si−H bond activation is participating in the "turnover-determining step".[48] These values are consistent with other small KIE values reported[12g,13c,49] for rate-limiting Si−H or C−H insertion reactions catalyzed by rhodium and copper reagents. The closely related hydride transfer from silanes to carbocations also provides modest experimental[50] or theoretically calculated KIE values[51] (from 1.1 to 2.7) for transition states varying widely in terms of Si−H (1.5−2.5 Å) and C−H (3.0−1.1 Å) distances as well as C−H−Si angles (129−180°). The higher end of the KIE value range (2.0−2.7) has been computationally achieved[51] for acute C−H−Si angles and late transition states.

The geometry of the transition state in H-transfer processes and possible elements of tunneling[52] have been occasionally assessed[53] by examining the temperature dependence of the KIE.[54] A plot of $\ln(k_H/k_D)$ as a function of 1/*T* based on the Arrhenius equation (eq 9) for an elementary reaction step provides ratios of Arrhenius preexponential factors A_H/A_D and differences of activation energies ($E_H - E_D$), which, according to

(45) Buschmann, H.; Scharf, H.-D.; Hoffmann, N.; Esser, P. *Angew. Chem., Int. Ed. Engl.* **1991**, *30*, 477−515.
(46) (a) Gypser, A.; Norrby, P.-O. *J. Chem. Soc., Perkin Trans. 2* **1997**, 939−943. (b) Hale, K. J.; Ridd, J. H. *J. Chem. Soc., Perkin Trans. 2* **1995**, 1601−1605.
(47) Palucki, M.; Finney, N. S.; Pospisil, P. J.; Güler, M. L.; Ishida, T.; Jacobsen, E. N. *J. Am. Chem. Soc.* **1998**, *120*, 948−954.
(48) Bosnich, B. *Acc. Chem. Res.* **1998**, *31*, 667−674.
(49) (a) Sulikowski, G. A.; Lee, S. *Tetrahedron Lett.* **1999**, *40*, 8035−8038. (b) Demonceau, A.; Noels, A. F.; Costa, J.-L. *J. Mol. Catal.* **1990**, *58*, 21−26. (c) Baer, T. A.; Gutsche, C. D. *J. Am. Chem. Soc.* **1971**, *93*, 5180−5186.
(50) (a) Mayr, H.; Basso, N.; Hagen, G. *J. Am. Chem. Soc.* **1992**, *114*, 3060−3066. (b) Chojnowski, J.; Fortuniak, W.; Stanczyk, W. *J. Am. Chem. Soc.* **1987**, *109*, 7776−7781.
(51) Apeloig, Y.; Merin-Aharoni, O.; Danovich, D.; Ioffe, A.; Shaik, S. *Isr. J. Chem.* **1993**, *33*, 387−402.
(52) Bell, R. P. *The Tunnel Effect in Chemistry*; Chapman and Hall: New York, 1981.
(53) Kwart, H. *Acc. Chem. Res.* **1982**, *15*, 401−408.
(54) Melander, L.; Saunders, W. H., Jr. *Reaction Rates of Isotopic Molecules*; Wiley-Interscience: New York, 1980; pp 44−45.

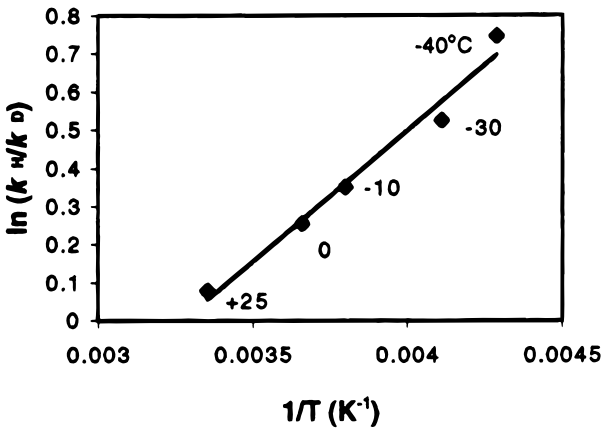

Figure 10. Arrhenius plot for the competitive carbenoid $PhC(N_2)CO_2Me$ insertion into the Si−H(D) bond of $PhMe_2$-Si-H/$PhMe_2$Si-D (1:1) mediated by $[Cu(CH_3CN)_4](PF_6)$ (10%)/*R*,*R*-**1** (12%) in CH_2Cl_2.

Kwart,[53] can be used as criteria to distinguish between linear and nonlinear (bent) H-transfer transition states. For instance, a bent transition state[53] for H-transfer is characterized by near temperature independence of KIE ($E_H - E_D \approx 0$) and an unusually high ratio of A_H/A_D (≥ 1.4). It has to be noted that the validity of these correlations has been questioned.[55] Especially high values of A_H/A_D have been suspected[55] to conceal mechanistic complexity rather than characterize an elementary step.

$$\ln(k_H/k_D) = \ln(A_H/A_D) - (E_H - E_D)/(RT) \qquad (9)$$

KIE values have been determined for the intermolecular carbenoid Si−H(D) insertion into $PhMe_2$Si-H/$PhMe_2$Si-D (1:1) at five different temperatures (−40, −30, −10, 0, +25 °C). A plot of $\ln(k_H/k_D)$ as a function of $1/T$ affords a reasonably linear correlation ($R^2 = 0.978$), from which values of A_H/A_D (0.11 ± 0.03) and $E_D - E_H$ (1.36 ± 0.12 kcal mol^{-1}) have been extracted. The value of A_H/A_D is not in the classical region for an elementary H/D-transfer step ($0.7 \leq A_H/A_D \leq 2^{1/2}$),[56] while the value of $E_D - E_H$ is substantially larger by comparison to the initial zero-point energy difference (ΔZPE = 0.87 kcal/mol) between $PhMe_2$Si-H ($\nu_{Si-H} = 2170$ cm^{-1}) and $PhMe_2$Si-D ($\nu_{Si-D} = 1560$ cm^{-1}), as determined by IR. Both A_H/A_D and $E_D - E_H$ values fall in a region that has been discussed in the literature[57] as indicative of tunneling effects (albeit also associated with high KIE values) in H-transfer mechanisms. However, due to the extrapolation involved (especially in the determination of A_H/A_D), the validity of the computed parameters needs to be further substantiated for a wider temperature region and a variety of silanes. Obviously, the possible interference of this quantum mechanical effect would not permit precise definition of the transition state.

Scheme 1

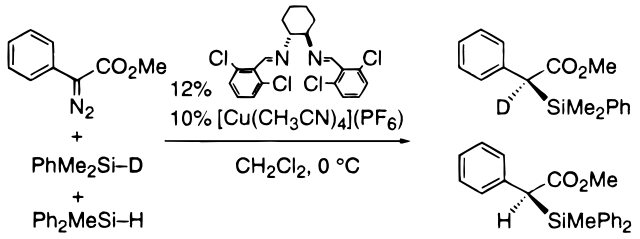

Unfortunately, all attempts toward further interrogating the timing of the transition state and the mode of Si−H activation (concerted insertion, radical H-atom abstraction, hydride transfer) by determining primary and most importantly secondary KIE values[50a,58] for Ph_2SiH_2, Ph_2SiHD, and Ph_2SiD_2 failed due to reduction of the catalyst to copper metal in the presence of dihydrosilanes.

(e) Control Experiments To Assess Possible Si−H Bond Cleavage Prior to Carbenoid Addition. The visible interaction of silanes with solutions of the copper catalyst in the absence of phenyl diazoacetate noted above raised the question whether copper hydrides,[59] formed via oxidative addition of silane[48] or by electrophilic hydride transfer to the copper site,[49a,60] may be involved in the catalytic reaction. Generation of a copper hydride reagent from the reaction of $PhMe_2$-SiH and CuCl in DMI (1,3-dimethylimidazolidinone) has been recently reported[61] to mediate conjugate reduction of α,β-unsaturated carbonyl compounds.

To evaluate the copper−hydride hypothesis as well as any other mechanistic scenario that requires cleavage of the Si−H bond prior to addition of the Si/H elements to the carbenoid carbon, we performed a number of control experiments. First, we note that the present catalytic system failed to mediate hydrosilation ($PhMe_2$-SiH) of acetophenone, a reaction that most likely depends on oxidative addition of the silane to the metal center.[2a,48,62] Most importantly, a catalytic reaction (Scheme 1) mediated by $[Cu^I(MeCN)_4](PF_6)$/*R*,*R*-**1**, involving $PhC(N_2)CO_2Me$ and a mixture of $PhMe_2$Si-D and Ph_2MeSi-H, showed no evidence of H/D scrambling (^{1}H NMR) in the insertion products $PhCD(SiMe_2Ph)CO_2Me$ and $PhCH(SiMePh_2)CO_2Me$ or in the remaining starting silanes. Furthermore, a carbenoid insertion reaction of $PhC(N_2)CO_2Me$ into $PhMe_2$Si-D in the presence of H_2 takes place without H atom enrichment of the C−D site in the product $PhCD(SiMe_2Ph)CO_2Me$.

These results strongly support the case for a concerted carbenoid Si−H insertion reaction. However, the possibility still exists that an initial hydride transfer to the

(55) Anhede, B.; Bergman, N.-Å. *J. Am. Chem. Soc.* **1984**, *106*, 7634−7636.
(56) Stern, M. J.; Weston, R. E., Jr. *J. Chem. Phys.* **1974**, *60*, 2808−2814.
(57) (a) Shaffer, M. W.; Leyva, E.; Soudararajan, N.; Chang, E.; Chang, D. H. S.; Capuano, V.; Platz, M. S. *J. Phys. Chem.* **1991**, *95*, 7273−7277. (b) Kim, Y.; Kreevoy, M. M. *J. Am. Chem. Soc.* **1992**, *114*, 7116−7123. (c) Bosch, E.; Moreno, M.; Lluch, J. M. *J. Am. Chem. Soc.* **1992**, *114*, 2072−2076. (d) Sorokin, A.; Robert, A.; Meunier, B. *J. Am. Chem. Soc.* **1993**, *115*, 7293−7299.
(58) (a) Merrigan, S. R.; Le Gloahec, V. N.; Smith, J. A.; Barton, D. H. R.; Singleton, D. A. *Tetrahedron Lett.* **1999**, *40*, 3847−3850. (b) Singleton, D. A.; Thomas, A. A. *J. Am. Chem. Soc.* **1995**, *117*, 9357−9358.
(59) (a) Mahoney, W. S.; Brestensky, D. M.; Stryker, J. M. *J. Am. Chem. Soc.* **1988**, *110*, 291−293. (b) Lipshutz, B. H.; Ung, C. S.; Sengupta, S. *Synlett.* **1989**, *1*, 64−66. (c) Tsuda, T.; Satomi, H.; Hayashi, T.; Saegusa, T. *J. Org. Chem.* **1987**, *52*, 439−443.
(60) (a) Sulikowski, G. A.; Cha, K. L.; Sulikowski, M. M. *Tetrahedron: Asymmetry* **1998**, *9*, 3145−3169. (b) Lee, S.; Lim, H.-J.; Cha, K. L.; Sulikowski, G. A. *Tetrahedron* **1997**, *53*, 16521−16532.
(61) Ito, H.; Ishizuka, T.; Arimoto, K.; Miura, K.; Hosomi, A. *Tetrahedron Lett.* **1997**, *38*, 8887−8890.
(62) (a) Noyori, R. *Asymmetric Catalysis in Organic Syntheses*; J. Wiley & Sons: New York, 1994. (b) Ojima, I. *Catalytic Asymmetric Syntheses*; VCH Publishers: Weinheim, Germany, 1993.

Scheme 2

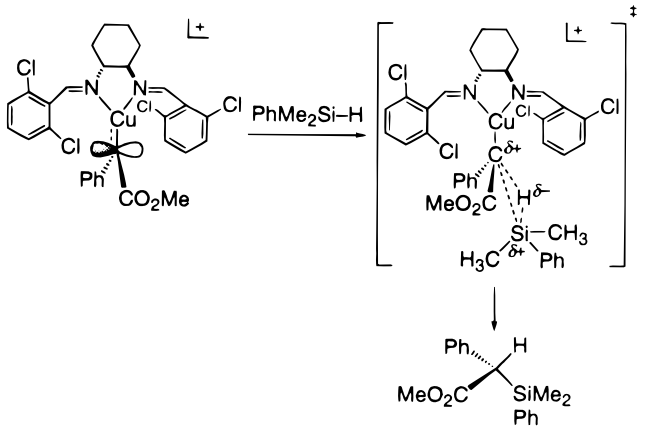

carbenoid carbon would generate a silicenium cation[63] either as part of the transition state (nonsynchronous concerted mechanism) or even as a discrete intermediate (two-step mechanism) which could then recombine with the carbon site prior to escaping. All attempts to capture a potential silicenium cation by virtue of F^- or $[BF_4]^-$ have been unsuccessful.[64]

Conclusions

Taken together, the mechanistic studies provide evidence to support a reaction pathway[65] characterized by (i) rate-limiting carbenoid insertion into the Si−H bond as suggested by the temperature-dependent KIE values; (ii) a concerted insertion of the carbenoid into the Si−H bond as invoked by control H/D scrambling experiments and suggested by the temperature dependence of the enantioselectivity (single-step enantioselection level); (iii) a polar transition state featuring positive charges on the carbon and to a lesser extent silicon atom (Hammett plots on reactivity); (iv) insensitivity of the levels of enantiocontrol with respect to the electronic properties of the carbenoid and silane moieties (Hammett plots on enantioselectivity), as well as in regards to the steric properties of the silanes; and (v) substantial dependence of ee values on the ligand characteristics and the presence of the phenyl substituent on the carbenoid moiety.

Although the evidence presented above cannot uniquely reconstrust the geometric features of the transition state, an attractive working hypothesis (Scheme 2) includes a hydrogen-first approach of the modestly polarized $Si^{\delta+}-H^{\delta-}$ vector toward the carbenoid carbon atom from the open side of the cavity and in a direction orthogonal to the electrophilic p-orbital residing on the carbon. An early transition state is preferred, featuring a rather wide C−H−Si angle, with the bulky silyl group positioned at the cavity's wide opening opposite the metal center. The early transition state better accommodates the insensitivity of ee values with respect to the steric requirements of the silanes and also accounts for the rather modest charge transfer from silicon to carbon in conjuction with H transfer and the significant entropic contribution to the energy difference of the diastereomeric transition states.

The good to high levels of enantiocontrol observed (usually associated with a late transition state) are most likely due to the characteristics of the copper carbenoid cavity, as dictated by the specific interactions of ligand moieties and the carbenoid. The structure of the cavity is thus considered to be sufficiently preorganized so that it could largely direct the trajectory of the Si−H approach toward the most favorable diastereotopic region. With the present combination of ligand and carbenoid precursor, this implies effective blockage of one side of the carbenoid moiety. In other combinations for which ee values have been shown[21] to drop precipitously, this steric restriction is lifted so that the approaching silane has the opportunity to effectively sample both sides of the carbenoid. Consistent with this notion of high specificity is the observation that the present catalyst system is also the most effective in asymmetric cyclopropanation (and aziridination) reactions. Further definition of the copper carbenoid structure is thus necessary to elucidate the origin of enantiocontrol. An additional point to be addressed in future studies is the stereochemistry of the C−Si bond formation in relation to Cu−C bond cleavage, which is expected[66] to proceed via inversion of the conformation of the incipient stereocenter developed upon hydride transfer to the carbenoid carbon.

Acknowledgment. We thank Profs. W. P. Giering and A. Prock for fruitful discussions, and Clementina Reyes for valuable experimental assistance. Financial support of this work by the U.S. Environmental Protection Agency (R823377-01-1 to P.S.) and the NIH/NCI (RO1 CA56304 to J.S.P.) is gratefully acknowledged. A James Flack Norris and Theodore William Richards Undergraduate Summer Scholarship (P.C.O) from the Northeastern Section of the American Chemical Society is also acknowledged.

Supporting Information Available: Analytical data for products of carbenoid insertions into Si−H bonds of silanes. ORTEP diagrams and Tables S1−S15 containing listings of crystal data and structure refinement, atomic coordinates and equivalent isotropic displacement parameters, interatomic distances and bond angles, anisotropic displacement parameters, and hydrogen coordinates and isotropic displacement parameters for compounds $[Cu^I(CH_3CN)_4](PF_6)\cdot CH_3CN$, **2**, and $[Cu^I{}_2(R,R\text{-}\mathbf{1})_3](PF_6)_2\cdot PhSCO_2Et\cdot 0.75CH_2Cl_2\cdot 0.5CH_3CN$. This material is available free of charge via the Internet at http://pubs.acs.org.

OM0003786

(63) (a) Reed, C. A. *Acc. Chem. Res.* **1998**, *31*, 325−332. (b) Maerker, C.; Schleyer, P. v. R. In *The Chemistry of Organic Silicon Compounds*; Rappoport, Z., Apeloig, Y., Eds.; John Wiley & Sons: New York, 1998; Vol. 2, Part 1, pp 513−555. (c) Lickiss, P. D. *Ibid*.; pp 557−594. (d) Lambert, J. B.; Zhao, Y. *Angew. Chem., Int. Ed. Engl.* **1997**, *36*, 400−401. (d) Olah, G. A.; Rasul, G.; Li, X.-Y.; Buchholz, H. A.; Sanford, G.; Prakash, G. K. S. *Science* **1994**, *263*, 983−984. (e) Pauling, L. *Science* **1994**, *263*, 983.

(64) Prakash, G. K. S.; Wang, Q.; Li, X.-y.; Olah, G. A. *New J. Chem.* **1990**, *14*, 791−792.

(65) For an early mechanistic analysis of dichlorocarbene insertion into Si−H bonds see: Seyferth, D.; Damrauer, R.; Mui, J. Y.-P.; Jula, T. F. *J. Am. Chem. Soc.* **1968**, *90*, 2944−2948.

(66) (a) Brookhart, M.; Liu, Y.; Goldman, E. W.; Timmers, D. A.; Williams, G. D. *J. Am. Chem. Soc.* **1991**, *113*, 927−939. (b) Brookhart, M.; Liu, Y. *J. Am. Chem. Soc.* **1991**, *113*, 939−944. (c) Casey, C. P.; Smith, L. J. *Organometallics* **1989**, *8*, 2288−2290.